https://doi.org/10.5194/cp-2019-89
Preprint. Discussion started: 9 August 2019


Climate of the Past
Discussions

# Evidence for a widespread climatic anomaly at around 7.5-7.0 cal ka BP

Mei Hou[1,2,5], Wenxiang Wu[1,2], David J. Cohen[3], Yang Zhou[1], Zhaoqi Zeng[1,5], Han Huang[1], Hongbo Zheng[4], and Quansheng Ge[1]

[1]Key Laboratory of Land Surface Pattern and Simulation, Institute of Geographical Sciences and Natural Resources Research, Chinese Academy of Sciences, Beijing 100101, China
[2]CAS Center for Excellence in Tibetan Plateau Earth Sciences, Beijing, 100101, China
[3]Department of Anthropology, National Taiwan University, Taipei, 10617, Taiwan, China
[4]Research Center for Earth System Science, Yunnan University, Kunming, 650091, China
[5]University of Chinese Academy of Sciences, Beijing, 100049, China

*Correspondence to:* Wenxiang Wu (wuwx@igsnrr.ac.cn)

**Abstract:** A climate event at 7.5–7.0 cal ka BP (1 cal ka BP=1000 calibrated years before present) has been recognized. This event is important for foreseeing the possible response of the climate system to global warming and for interpreting considerable societal change, but it has heretofore lacked a systematic review. Here, we summarize previously published paleoclimate records spanning this event from 47 sites around the world. The proxy evidence from a variety of paleo-archives, including lake sediment, speleothem, marine sediment, and ice core, provides a clear picture of this climate change. The synthesis results show a weaker Asian summer monsoon, in contrast to a stronger South American summer monsoon during the event. The event also involves dramatic cooling and wetter conditions in north-central Europe and in western North America, widespread aridity across Africa, contrasting patterns of precipitation variability throughout the Mediterranean, and notable cooling over the polar region, suggesting that it is a worldwide climate event. Comparison of paleoclimate records with climate-forcing time series gives likely climate controls for the event. The close correspondence in time of solar irradiance minima, strong volcanic eruptions, the meltwater flux into the North Atlantic, an orbitally induced decrease in solar insolation, and climate changes indicated by proxy data suggest

https://doi.org/10.5194/cp-2019-89
Preprint. Discussion started: 9 August 2019


Climate of the Past Discussions

possible linkages. More quantitative reconstructions and higher resolution climate records are needed to fully capture the magnitude, timing, duration, and nature of this event, which will be of considerable relevance to modeling.

**Keywords:** Holocene; 7.5–7.0 cal ka BP event; proxy record; causal mechanisms

## 1 Introduction

Future climate change and its potential effects on human society and ecosystems are of prime concern to all. Climate modeling suggests that human-induced forcings are increasing the probability of abrupt climate changes in the next hundred years or beyond (National Research Council, 2002; IPCC, 2013). One way to quantify the possible impact of future abrupt climate change is to look to the past for possible close analogs (Alley and Ágústsdóttir, 2005). The Holocene was interrupted by a number of abrupt climate changes at decade-to-century time scales, which typically occurred at times when the background climate was much like the present (Bond et al., 2001; Mayewski et al., 2004; Wang et al., 2005; Shuman, 2012). Studies of such episodes can provide insight into the process, driver, and effect of abrupt climate change, which can then be applied to understand the behavior of climate systems and thus to deal with the likely occurrence of future abrupt climate change. Our consideration of paleoclimatic records first focuses attention on an 8.2 cal ka BP (thousand calibrated years before present) event (Alley et al., 1997; Alley and Ágústsdóttir, 2005), a 5.5 cal ka BP event (Brooks, 2006; Wu et al., 2018), and a 4.2 cal ka BP event (Wu and Liu, 2004; Roberts et al., 2011; Weiss, 2016), which have been strongly detected in a range of different types of paleoclimate archives.

With the application of multi-proxy studies and tightly constrained dating controls, the quantity of paleoclimate records has increased, making it possible to recognize a series of minor oscillations in the signatures of Holocene climate change. One such climatic shift occurred at approximately 7.5–7.0 cal ka BP when paleoclimate records from the North Atlantic (Bond et al., 2001), the Mediterranean (Magny et al., 2013; Cheng et al., 2015), Asia (Yu et al., 2004; Gupta et al., 2005;

https://doi.org/10.5194/cp-2019-89
Preprint. Discussion started: 9 August 2019


Wang et al., 2005; Liu et al., 2015), the Americas (Ersek et al., 2012; Bernal et al., 2016), Europe, and Africa (Thompson et al., 2002; Magny, 2004; Magny et al., 2011; Zielhofer et al., 2017) show multicentennial climatic event signals. This climate shift is also visible in a few polar ice core records (Stuiver et al., 1995; Mayewski et al., 1997). This event has been referred to in various ways related to its chronology, including as the 7.1 ka event (Aubán et al., 2015), the 7.4 ka event (Fletcher et al., 2012), and the ice-rafted debris (IRD)-5b event (Gronenborn, 2010), although here we refer to it as the 7.5–7.0 cal ka BP event. The available data suggest that the 7.5–7.0 cal ka BP event is characterized by climate changes of smaller amplitude than those of widely acknowledged climate events. Nonetheless, this climate event is particularly interesting because it occurs during the Holocene Climate Maximum, when the climate was similar to or even warmer than recently, so it may provide useful estimates concerning potential limits on the magnitude of climate changes possible in the future.

In addition, the interval of 7.5–7.0 cal ka BP represented by this event coincides with significant changes seen archaeologically in human societies throughout the world. It was a period of settlement pattern changes such as the abandonment of a large number of sites, demographic shifts, and profound cultural transformations (Shi et al., 1994; Aubán et al., 2015). The transition from the Mesolithic to the Neolithic across southern Iberia and the final collapse of the Early Neolithic Linear Pottery culture across central Europe were associated with climatic instability and resulted in changes to subsistence strategies at around 7.4 cal ka BP (Gronenborn, 2010; Sánchez et al., 2012). In China, climatic deterioration between 7.5 and 7.0 cal ka BP coincided with considerable regional Neolithic cultural successions, particularly in the northerly latitudes, including those now recognized across the Guanzhong Basin (Lü and Zhang, 2008), the Gansu-Qinghai region (Dong, 2013), the farming–grazing transitional zone (Zhang et al., 1997), and North China (Wang et al., 2014). The correlation of archaeological evidence for such cultural changes with the 7.5–7.0 cal ka BP event leads us to hypothesize that climate change in this period had significant yet variable impacts on human societies across the globe. Demonstrating climate change as a

https://doi.org/10.5194/cp-2019-89
Preprint. Discussion started: 9 August 2019




causative factor in these geographically widespread cultural changes, however, will require greater systematic knowledge about the event as well as about the archaeological changes at the regional level; we may then more fully evaluate the impacts of this climate event on the development of human societies.

For these reasons, it is necessary to have a detailed understanding of the 7.5–7.0 cal ka BP event. Here, we do this through the synthesis of paleoclimate proxy records from various archives from different areas, which have become more plentiful in recent decades. The use of widely distributed site-specific paleoclimatic data avoids the risk of using data series from one area to extrapolate to others and thus provides a more reliable picture of the 7.5–7.0 cal ka BP event (Shuman and Marsicek, 2016). In this article, we synthesize well-dated and highly-resolved climate records from 47 globally distributed sites spanning the time range of the 7.5–7.0 cal ka BP event. The aim of this synthesis is not only to compile high-quality data, but also to understand the temporal and spatial pattern of this climate change and to investigate the underlying climate-forcing mechanisms and the resulting impacts of the climatic change. These in turn can be used as a basis for interpreting regional archaeological records and for testing and validating general circulation models used to predict future climate.

## 2 Site Selection

Advances in paleoclimatic research have led to the publication of a large number of Holocene paleoclimatic records in the last decades. Here, we concentrate on published records of climate change associated with the interval of 7.5–7.0 cal ka BP. We exclude those records that do not provide convincing evidence of an event across this interval; hence, this review is not exhaustive. We are interested in records characterized as follows: (1) the record covers the entire time interval of interest; (2) the proxies measured have a demonstrated relationship with climate variables; (3) the records have a reliable chronological framework and high resolution (i.e., to ensure the credibility of review results, a record should have a sampling resolution of better than 200 years and at least one control point every 2,000 years; a low resolution does not allow us to identify shorted-lived, multicentennial cold or warm periods); and (4)

https://doi.org/10.5194/cp-2019-89
Preprint. Discussion started: 9 August 2019




the record is preferably multi-proxy (given that different proxies from the same record can yield different inferences about the timing and magnitude of climatic change). In many, but far from all, of the records, a variety of different proxies are included to provide accurate paleoclimate and paleoenvironment information for the 7.5–7.0 cal ka BP event. With respect to the four criteria, 47 sites are presented in this review: 13 lake sediments, 12 speleothems, 16 marine sediments, and 6 ice cores. Individual data sets cannot detect all regionally significant changes because any given change may be spatially heterogeneous and may not affect all sites. Similarly, any individual proxy record cannot represent the full complexity of the climate change. Our site-selection criteria allowed us to use multi-site, multi-proxy analyses as a way to improve reliability and confidence in the paleoclimate signals. We suggest that our approach provides a useful framework through which the character of the 7.5–7.0 cal ka BP event can be assessed. Because of the complex relationship between climate variables and proxies, it is impossible to translate each individual proxy into quantitative or semiquantitative climate signals. Therefore, in some cases, we have followed the authors' original interpretations of the paleoclimate records and have not made any corrections.

The details of the paleoclimate records discussed in this review are listed with the type of archive, dating material, number of dates, dating method, resolution, and proxy type in Table 1. Record locations are plotted on a map of the world to help visualize their spatial distribution (Fig. 1). Because the various proxies have been dated by different techniques, all ages in this text are given as calibrated ages, with the notation "cal ka BP," to provide a common chronological framework for comparison.

For ease of discussion, the 47 sites are grouped into five regions: Asia, the Americas, Europe and the Mediterranean, Africa, and the polar region. In addition, several records indicating sea-level changes are introduced separately. We present 40 proxy time series from these regions and 6 additional climate-forcing time series. Numeric data for these proxies were downloaded either from the National Oceanic and Atmospheric Administration (https://www.ncdc.noaa.gov/data-access/

https://doi.org/10.5194/cp-2019-89
Preprint. Discussion started: 9 August 2019

Climate of the Past Discussions
Open Access

paleoclimatology-data) or as digitized figures produced with GetData2.20 software (http://www.getdata-graph-digitizer.com/).

https://doi.org/10.5194/cp-2019-89
Preprint. Discussion started: 9 August 2019




**Table 1.** Details for the proxy records reviewed in this study

| No. | Site | Longitude | Latitude | Archive | Dating material | No. of dates | Dating method | Resolution (yr) | Proxy | Reference |
|---|---|---|---|---|---|---|---|---|---|---|
| 1 | Dongge | 108.50 | 25.17 | cave | stalagmite | 45 | U-TH | 5 | $\delta^{18}O$ | Wang et al., 2005 |
| 2 | Qingtian | 110.22 | 31.20 | cave | stalagmite | 31 | U-TH | 2–6 | $\delta^{18}O$ | Liu et al., 2015 |
| 3 | Tianmen | 90.40 | 30.55 | cave | stalagmite | 15 | U-TH | 3–7 | $\delta^{18}O$ | Cai et al., 2012 |
| 4 | Qinghai Lake | 100.08 | 36.32 | lake | organic matter/seed/ plant macrofossils | 57 | AMS$^{14}$C | 56 | monsoon index | An et al., 2012 |
| 5 | Ximenglongtan | 99.35 | 22.38 | lake | plant macrofossils | 12 | AMS$^{14}$C | 10–20 | geochemistry | Ning et al., 2017 |
| 6 | Dajiuhu | 110.00 | 31.28 | peat | organic matter | 14 | AMS$^{14}$C | 65 | biomarker | Huang et al., 2013 |
| 7 | Yellow Sea | 122.55 | 39.24 | sea core | organic matter | 10 | AMS$^{14}$C | 55 | alkenones | Nan et al., 2017 |
| 8 | Daihai | 112.40 | 40.35 | lake | organic matter | 9 | AMS$^{14}$C | 23–158 | pollen | Xu et al., 2003 |
| 9 | Dunde | 96.25 | 38.06 | ice core | ice | — | ice counting | — | $\delta^{18}O$ | Thompson et al., 1989 |
| 10 | Guliya | 81.29 | 35.17 | ice core | ice | — | ice counting | — | $\delta^{18}O$ | Thompson et al., 1997 |
| 11 | Leizhou Peninsula | 109.55 | 20.14 | sea core | reef | 9 | AMS$^{14}$C | sub-annual | Sr/Ca | Yu et al., 2004 |
| 12 | Arabian Sea | 57.36 | 18.03 | sea core | foraminifer | 15 | AMS$^{14}$C | 30 | planktic foraminifer | Gupta et al., 2005 |
| 13 | Hoti | 57.21 | 23.05 | cave | stalagmite | 12 | U-TH | 4 | $\delta^{18}O$ | Neff et al., 2001 |
| 14 | Qunf | 54.18 | 17.10 | cave | stalagmite | 18 | U-TH | 4–5 | $\delta^{18}O$ | Fleitmann et al., 2003 |
| 15 | Mawmluh | 91.52 | 25.15 | cave | stalagmite | 12 | U-TH | 5 | $\delta^{18}O$ | Berkelhammer et al., 2012 |
| 16 | Oregon | –123.25 | 42.05 | cave | stalagmite | 29 | U-TH | 3 | $\delta^{18}O$ | Ersek et al., 2012 |
| 17 | Pink Panther | –105.17 | 32.08 | cave | stalagmite | 22 | U-TH | 17 | $\delta^{18}O$ | Asmerom et al., 2007 |
| 18 | Soledad Basin | –112.70 | 25.20 | sea core | foraminifer | 22 | AMS$^{14}$C | 50 | Mg/Ca | Marchitto et al., 2010 |
| 19 | Florida Straits | –83.13 | 24.24 | sea core | foraminifer | 7 | AMS$^{14}$C | 25 | planktic foraminifera | Schmidt et al., 2012 |
| 20 | Nordan's Pond | –53.36 | 49.90 | peat | plant macrofossils | 10 | AMS$^{14}$C | ~100 | composite proxy | Hughes et al., 2006 |
| 21 | Botuverá | –49.09 | –27.13 | cave | stalagmite | 13 | U-TH | sub-annual | $\delta^{18}O$ | Bernal et al., 2016 |
| 22 | Lapa Grande | –44.21 | –14.25 | cave | stalagmite | 24 | U-TH | 10 | $\delta^{18}O$ | Str kis et al., 2011 |
| 23 | Titicaca | –69.26 | –15.57 | lake | organic matter | 9 | AMS$^{14}$C | 45 | $\delta^{13}C$ | Baker et al., 2005 |
| 24 | El Junco Lake | –91.00 | –0.30 | lake | organic matter | 21 | AMS$^{14}$C | 5–50 | botryococcenes | Zhang et al., 2014 |
| 25 | North Atlantic | –14.43 | 55.28 | sea core | foraminifer | 59 | AMS$^{14}$C | 40 | hematite-stained grains | Bond et al., 2001 |
| 26 | Faroe Islands | 61.61 | –5.53 | sea core | foraminifer | 5 | AMS$^{14}$C | 20–80 | benthic and planktic foraminifera | Rasmussen and Thomsen, 2010 |
| 27 | Lake Tsuolbmajavri | 22.05 | 68.41 | lake | plant macrofossils | 14 | AMS$^{14}$C | 50–70 | diatom | Korhola et al., 2000 |
| 28 | Lago Preola | 12.38 | 37.37 | lake | peat | 8 | AMS$^{14}$C | 64 | sedimentological analyses | Magny et al., 2011 |
| 29 | MD04-2797CQ | –11.40 | 36.57 | sea core | foraminifer | 13 | AMS$^{14}$C | 100 | pollen | Desprat et al., 2013 |
| 30 | Accesa | 10.53 | 42.59 | lake | plant macrofossils/ tephra layer | 17 | AMS$^{14}$C | 50 | sediment lithology | Magny et al., 2007 |
| 31 | Adriatic Sea | 17.37 | 41.17 | sea core | foraminifera | 10 | AMS$^{14}$C | 40 | $\delta^{18}O$ | Siani et al., 2013 |
| 32 | MD99-2343 | 4.01 | 40.29 | sea core | foraminifera | 8 | AMS$^{14}$C | 150 | planktic foraminifer | Frigola et al., 2007 |
| 33 | MD95-2043 | –2.37 | 36.90 | sea core | foraminifera | 9 | AMS$^{14}$C | 100 | pollen | Fletcher et al., 2012 |
| 34 | Padul Lake | –3.36 | 37.00 | lake | plant remains | 17 | AMS$^{14}$C | 65 | pollen | Ramos-Román et al., 2018 |
| 35 | Soreq | 35.03 | 31.45 | cave | stalagmite | 53 | U-TH | 40 | $\delta^{18}O$ | Bar-Matthews et al., 1999 |
| 36 | Jeita | 35.39 | 33.57 | cave | stalagmite | 63 | U-TH | 7 | $\delta^{18}O$, $\delta^{13}C$, Sr/Ca | Cheng et al., 2015 |
| 37 | Nile delta | 29.27 | 31.47 | sea core | foraminifera | 17 | AMS$^{14}$C | 10 | geochemistry | Revel et al., 2010 |
| 38 | Lake Sidi Ali | –5.00 | 33.03 | lake | plant macrofossils/ pollen | 26 | AMS$^{14}$C | 100 | geochemistry | Zielhofer et al., 2017b |
| 39 | Kilimanjaro | 37.21 | –3.04 | ice core | ice | — | tuning | 50 | dust flux | Thompson et al., 2002 |
| 40 | GISP2 | –38.50 | 72.60 | ice core | ice | — | layer counting | 0.5–2.5 | $Na^+$, $K^+$, $Ca^{2+}$ | Mayewski et al., 1997 |
| 41 | Taylor Dome | 158.43 | –77.47 | ice core | ice | — | tuning | 7 | $\delta^{18}O$ | Steig et al., 2000 |
| 42 | GRIP | –37.37 | 72.34 | ice core | ice | — | glaciological | 85 | $CH_4$ | Blunier et al., 1995 |
| 43 | Baltic Sea | 15.04 | 56.11 | sea core | plant macrofossils/ organic matter | 65 | AMS$^{14}$C | — | sedimentary facies | Yu et al., 2007 |
| 44 | Yellow Sea | 120.31 | 37.47 | sea core | peat | — | AMS$^{14}$C | — | sea level | Liu et al., 2004 |
| 45 | Kuahuqiao | 120.13 | 30.12 | cultural sediment | organic matter/plant macrofossils/charcoal | 11 | AMS$^{14}$C | 40 | pollen | Zong et al., 2007 |
| 46 | Singapore | 103.89 | 1.30 | sea core | wood/shell | 15 | AMS$^{14}$C | — | sea level | Bird et al., 2010 |
| 47 | Grand Cayman | –81.04 | 19.19 | sea core | reef | 9 | U-TH | — | sea level | Blanchon et al., 2002 |

https://doi.org/10.5194/cp-2019-89
Preprint. Discussion started: 9 August 2019



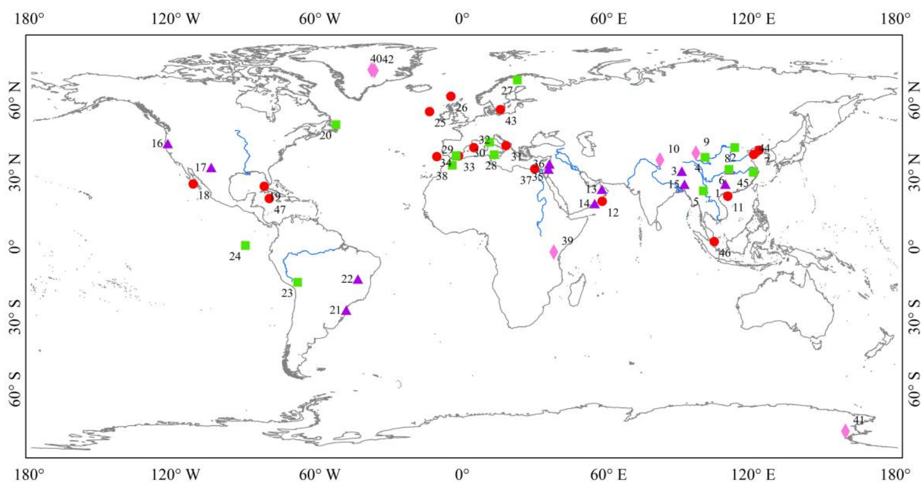


**Figure 1.** Map of the site locations reviewed. The different symbols represent different types of paleoclimatic archives (violet triangle: speleothem; magenta diamond: ice core; green square: lake sediment; red circle: marine sediment).

## 3 Proxy Records

In the following descriptions, we present relevant evidence from the various proxy records across the five regions. Location numbers of the sites shown in Figure 1 are indicated in parentheses after each reference.

### 3.1 Asia

The growing number of proxy records from the Asian summer monsoon domain, ranging from the beginning to the end of the Holocene, allows for good analysis of past climate change in the region. For the region of Asia, one area with a relatively high concentration of sites is associated with China. In southern China, a $\delta^{18}O$ record at a 5-year sampling resolution from an absolute-dated speleothem from the Dongge Cave showed a century-scale sharp anomaly centered at 7.2 cal ka BP (Wang et al., 2005; Fig. 2m) (1). In central China, a speleothem record with a temporal resolution of 2 to 6 years from Qingtian Cave in the Shennongjia Mountains, revealed a very fast onset event, with a marked anomaly in oxygen-isotopic composition between 7.4 and 7.2 cal ka BP (Liu et al., 2015; Fig. 2k) (2). Further west, in the southern Tibetan Plateau, a $\delta^{18}O$ record at a 3- to 7-year sampling resolution from a precisely dated speleothem from Tianmen Cave indicated a prominent oxygen-isotopic shift to

https://doi.org/10.5194/cp-2019-89
Preprint. Discussion started: 9 August 2019




positive values centered at 7.3 cal ka BP (Cai et al., 2012; Fig. 2l) (3). The $\delta^{18}O$ value shift in these three stalagmite records revealed a major climatic change between 7.5 and 7.0 cal ka BP, with their heavier values reflecting a weaker summer monsoon. Additional evidence for a weakened monsoon is apparent in two lacustrine records. One multi-proxy record from Qinghai Lake in the northeastern Tibetan Plateau is constrained by 57 accelerator mass spectrometry (AMS) $^{14}C$ ages on terrestrial plant remains and bulk organic matter (An et al., 2012; Fig. 2e) (4). The low $CaCO_3$ content and total organic carbon flux together likely point to a dry climate condition at 7.5–7.0 cal ka BP, which is supported by an enriched ostracod $\delta^{18}O$ value, a proxy for the precipitation–evaporation budget (An et al., 2012). The other record comes from Lake Ximenglongtan in southwestern China, where well-dated, high-resolution geochemical and grain-size data showed a pronounced and prolonged drought interval between 7.5 and 7.0 cal ka BP (Ning et al., 2017) (5).

Several reconstructions of temperature have been made through the interval of 7.5–7.0 cal ka BP. Collectively, these records provide strong evidence for a greatly reduced temperature. A microbial lipid-based annual temperature reconstruction from the Dajiuhu peatland suggested temperatures about 2–3 °C colder than previously from 7.5 to 7.0 cal ka BP (Huang et al., 2013; Fig. 2i) (6). To the north, Daihai Lake, at the present marginal zone of the East Asian summer monsoon, is sensitive to climate changes. Robust quantitative estimates of the Holocene climate using a pollen-based model indicated a sharp cooling in an inferred July temperature of roughly 2 °C between 7.6 and 7.4 cal ka BP (Xu et al., 2003; Fig. 2j) (8). Note also that an abrupt depletion in $\delta^{18}O$ values in the Dunde ice core provided reliable evidence of a transition toward colder conditions at approximately 7.3 cal ka BP (Thompson et al., 1997; Fig. 2g) (9). A gradual increase in $\delta^{18}O$ values since 7.5 cal ka BP was recorded in the Guliya ice core, suggesting analogous cooling (Thompson et al., 1989; Fig. 2f) (10). A climate shift that characterizes the event was clearly identified on the Leizhou Peninsula in the northern South China Sea, where an annually resolved Sr/Ca-based temperature reconstruction from a *Goniopora* reef

https://doi.org/10.5194/cp-2019-89
Preprint. Discussion started: 9 August 2019

Climate of the Past Discussions

profile suggested a winter temperature 2–3 °C colder than present between 7.5 and 7.0 cal ka BP (Yu et al., 2004) (11). This result was strongly supported by microstructural examination of the *Goniopora* skeletons, which revealed at least nine massive, abrupt *Goniopora* mortality events resulting from winter cooling. In the northern Yellow Sea, a reconstruction of relative sea surface temperature (SST) changes, based on long-chain unsaturated alkenones, suggested that a cold event featuring reductions in the summer SST of 3–4 °C was recorded between 7.2 and 7.0 cal ka BP (Nan et al., 2017; Fig. 2h) (7). This cold event could have been caused by an abrupt decrease in the strength of the Kuroshio Current, a signal that was recently discovered in sediment from the western slope of the northern Okinawa Trough (Zheng et al., 2016). Shi et al. (1994), in an review of widely distributed paleoclimate records from China, including paleosols, palynology, paleolimnology, and ice core, found a pronounced cold event at 7.3 cal ka BP.

A broad Holocene monsoon minimum between 7.5 and 7.0 cal ka BP is also found in the Indian summer monsoon domain. The most important records are perhaps those from offshore Oman. The percentage concentrations of fossil shells of the planktic foraminifer *G.bulloides* derived from a marine sediment core from the northwestern Arabian Sea off Oman showed a distinct low between 7.5 and 7.3 cal ka BP (Fig. 2c), indicative of a summer monsoon minimum (Gupta et al., 2005) (12). The data paralleled the short-term variations in the speleothem $\delta^{18}O$ record of Hoti Cave in northern Oman, which indicated a decrease in rainfall at 7.5–7.2 cal ka BP (Neff et al., 2001; Fig. 2d) (13), whereas a gradual increase in oxygen isotopes of a speleothem from Qunf Cave in southern Oman indicated the development of drier conditions after 7.5 cal ka BP under a weakening of the summer monsoon (Fleitmann et al., 2003; Fig. 2a) (14). To the east, the highly resolved speleothem $\delta^{18}O$ data of Berkelhammer et al. (2012) (15) from the Mawmluh Cave in northeastern India showed a prominent shift to heavier values, indicating a monsoon reduction between 7.3 and 7.0 cal ka BP (Fig. 2b).

Overall, multiple speleothem records from the Asian monsoon domain have

https://doi.org/10.5194/cp-2019-89
Preprint. Discussion started: 9 August 2019




rather clearly shown a well-defined reduction in monsoon intensity between about 7.5 and 7.0 cal ka BP. This result is supported by other lines of proxy evidence from the lacustrine records and marine records. Most temperature-sensitive proxies show a typical sharp, cold signature but one that is abrupt and that caused non-reversing cooling.

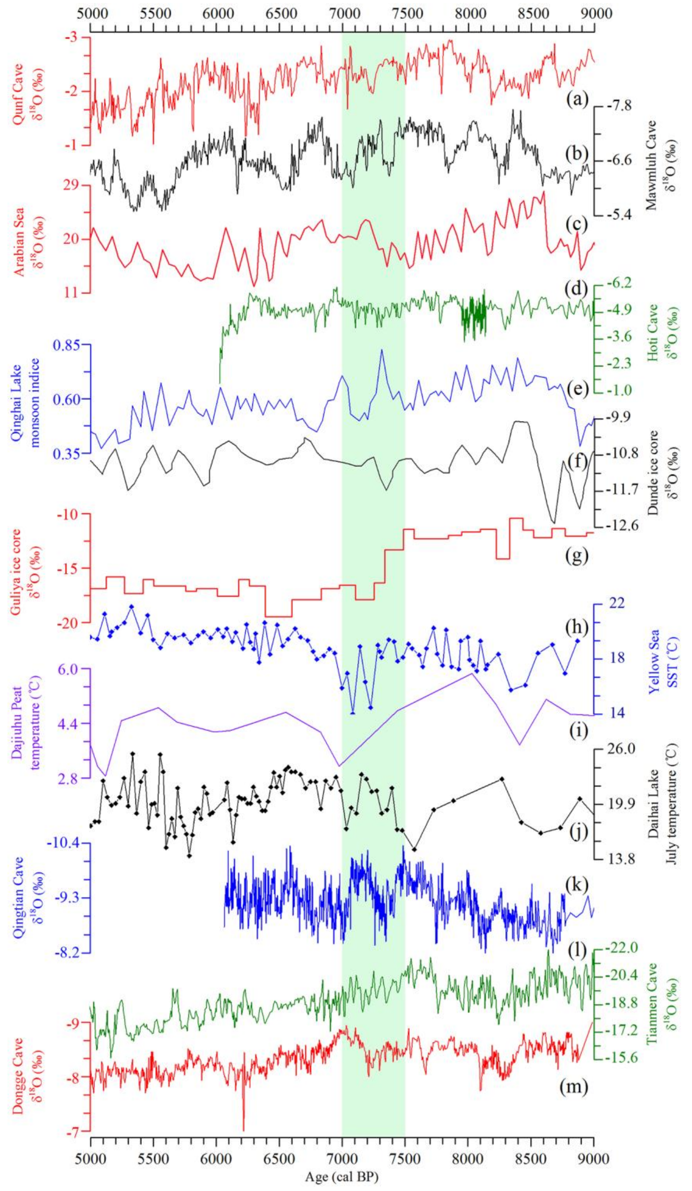


**Figure 2.** Proxy time series for the Asian summer monsoon domain. (a) Stalagmite

$\delta^{18}O$ for Qunf Cave, southern Oman (Fleitmann et al., 2003). (b) Stalagmite $\delta^{18}O$ for Mawmluh Cave, northeastern India (Berkelhammer et al., 2012). (c) Percentage of *Globigerina bulloides* for the Arabian Sea (Gupta et al., 2005). (d) Stalagmite $\delta^{18}O$ for Hoti Cave, northern Oman (Neff et al., 2001). (e) A composite summer monsoon index for Qinghai Lake, northeastern Tibetan Plateau (An et al., 2012). (f) $\delta^{18}O$ for the Dunde ice core, northeastern Tibetan Plateau (Thompson et al., 1989). (g) $\delta^{18}O$ for the Guliya ice core, western Tibetan Plateau (Thompson et al., 1997). (h) A sea surface temperature (SST) reconstruction for the Yellow Sea (Nan et al., 2017). (i) An annual temperature reconstruction for the Dajiuhu Peat (Huang et al., 2013). (j) A July temperature reconstruction for Daihai Lake (Xu et al., 2003). (k) Stalagmite $\delta^{18}O$ for Qingtian Cave, central China (Liu et al., 2015). (l) Stalagmite $\delta^{18}O$ for Tianmen Cave, southern Tibetan Plateau (Cai et al., 2012). (m) Stalagmite $\delta^{18}O$ for Dongge Cave, southern China (Wang et al., 2005).

### 3.2 The Americas

Beginning in western North America, Ersek et al. (2012) (16) provided a high-resolution speleothem record from a cave in southwestern Oregon, USA. Significant anomalies in the carbon and oxygen isotopes at 7.4 cal ka BP (Fig. 3c) are likely explained in terms of isotopic changes in wintertime precipitation, with light $\delta^{18}O$ values reflecting colder conditions and negative $\delta^{13}C$ values corresponding to increased precipitation. Similarly, Asmerom et al. (2007) (17) noted prominent negative $\delta^{18}O$ excursions of a speleothem from the Pink Panther Cave in New Mexico, USA, possibly suggesting a strong increase in precipitation from 7.3 to 7.0 cal ka BP (Fig. 3b). To the northeast, Hughes et al. (2006) (20) analyzed plant macrofossils, testate amoebae, and peat humification in a peat profile from eastern Newfoundland, Canada, which suggested colder and more humid conditions between 7.5 and 7.0 cal ka BP (Fig. 3a). The authors suggest that the low temperatures restrict surface evaporation and would explain a wetter climate well at this time. Further south, in the eastern tropical Pacific, Marchitto et al. (2010) (18) reported a cool interval recorded by a Mg/Ca-based reconstruction of the SST from off the west coast

https://doi.org/10.5194/cp-2019-89
Preprint. Discussion started: 9 August 2019



of the Baja California Sur in Mexico between 7.2 and 7.0 cal ka BP (Fig. 3e). In a high-time-resolution marine-sediment core from the Florida Straits, Schmidt et al. (2012) (19) found a period of increased sea surface salinity based on $\delta^{18}O$ of *Globigerinoides ruber* at 7.6 to 7.4 cal ka BP (Fig. 3d), which they associated with an increased evaporation/precipitation ratio and more arid conditions. Viau et al. (2006) completed an important reconstruction of July temperature from 752 fossil pollen records distributed across North America by using the modern analog technique, which revealed a cold interval centered at 7.5 cal ka BP. Mountain glaciers are sensitive indicators of environmental change and are likely to provide additional support for cooler temperatures. Menounos et al. (2009) summarized multi-proxy evidence of Holocene glacial fluctuations in the Canadian Cordillera and found a glacial advance between 7.4 and 7.0 cal ka BP, which Ryder and Thomson (1986) referred to as the "Garibaldi Phase."

Paleoclimate records covering the interval of interest are rare in the South American monsoon sector. Nevertheless, available speleothem and lake records suggest an intensification of monsoon precipitation from 7.5 to 7.0 cal ka BP. Bernal et al. (2016) (21) presented evidence, on the basis of the decreased Sr/Ca ratios and 0.5 per mil shift in the $\delta^{18}O$ value of a speleothem from Botuverá Cave in southeastern Brazil, for increased precipitation centered at 7.2 cal ka BP (Fig. 3g). Similarly, Strίkis et al. (2011) (22) found an anomaly in the oxygen-isotopic composition of a speleothem of about 1 per mil toward negative values in the Lapa Grande Cave in central-eastern Brazil, which was thought to be coincident with an increase in rainfall around 7.5–7.3 cal ka BP. Further west, Baker et al. (2005) (23) measured the carbon-isotopic content of bulk organic matter to reconstruct the lake-level history of Lake Titicaca on the Altiplano of Bolivia and Peru. From 7.5 to 7.0 cal ka BP, the $\delta^{13}C$ showed a distinct shift toward more negative values (Fig. 3f), indicating a sharp increase in rainfall and a high lake level. Recently, in a high-time-resolution sediment core from El Junco Lake in the Galápagos Islands, Zhang et al. (2014) (24) used concentration and hydrogen isotope ratio of lipids

https://doi.org/10.5194/cp-2019-89
Preprint. Discussion started: 9 August 2019



produced by the green alga *Botryococcus braunii*, which is linked to precipitation variability in response to the El Niño, to infer a clear increase in El Niño activity between 7.6 and 7.4 cal ka BP. Further south in southernmost South America, Pérez-Rodríguez et al. (2016) noted low Zr accumulation rates, indicating relatively dry conditions centered at 7.2 cal ka BP in sediment from Lago Hambre. In the same region, Menounos et al. (2013) combined AMS$^{14}$C dating of several leaves between two moraines with the age of Hudson tephra beyond the moraines, demonstrating a mountain glacial advance in southernmost Tierra del Fuego, Argentina, at that time.

The 7.5–7.0 cal ka BP event rather clearly affected eastern Newfoundland in Canada, western North America, Mexico, and into Brazil and Peru. Climate anomalies associated with the event included cool and wet conditions across western North America and increased monsoon rainfall in South America. Paleoclimate proxy records are particularly needed from eastern North America and the U.S. Great Plains.

https://doi.org/10.5194/cp-2019-89
Preprint. Discussion started: 9 August 2019




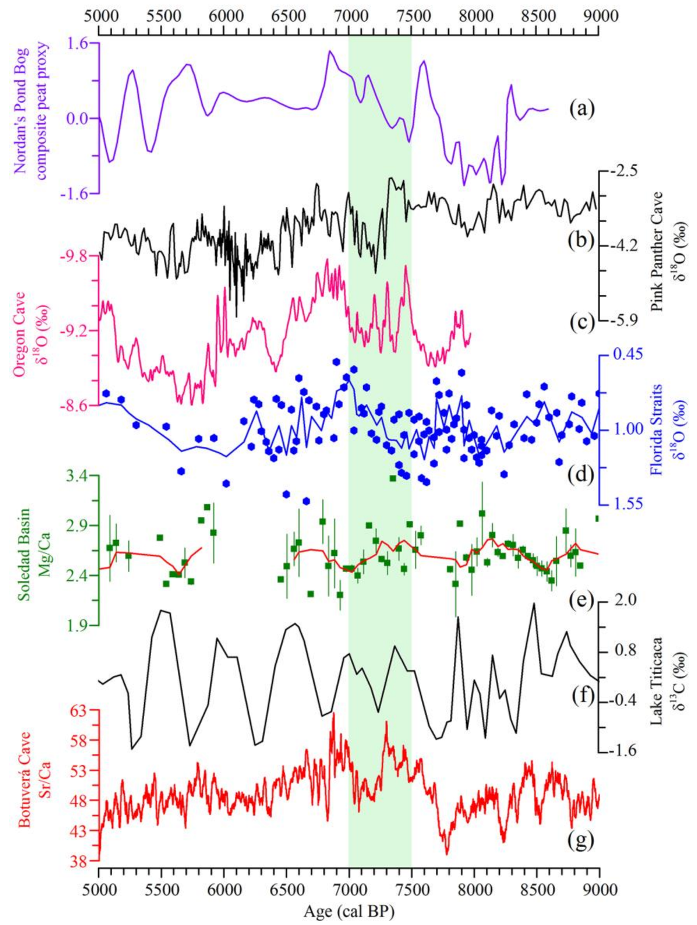


**Figure 3.** Proxy time series for the Americas. (a) Composite bog proxies for Nordan's Pond Bog, Canada (Hughes et al., 2006). (b) Stalagmite $\delta^{18}$O for Pink Panther Cave, USA (Asmerom et al., 2007). (c) Stalagmite $\delta^{18}$O for Oregon Cave, USA (Ersek et al., 2012). (d) Calculated ice volume free $\delta^{18}O_{SW}$ ($\delta^{18}O_{IVF\text{-}SW}$) record for the Florida Straits, USA (Schmidt et al., 2012). (e) Mg/Ca ratios for Soledad Basin, Mexico (Marchitto et al., 2010). (f) $\delta^{13}$C for Lake Titicaca, Altiplano of Bolivia and Peru (Str ķis et al., 2011). (g) Sr/Ca ratio for Botuverá Cave, Brazil (Bernal et al., 2016).

### 3.3 Europe and the Mediterranean

Throughout this region, a particularly revealing case is portrayed by high-resolution drift-ice records from North Atlantic sediment cores. The records

https://doi.org/10.5194/cp-2019-89
Preprint. Discussion started: 9 August 2019




documented nine peaked events in the IRD during the Holocene, one of which occurred between around 7.5 and 7.3 cal ka BP (Bond et al., 2001; Fig. 4a) (25), which Gronenborn (2010) termed the "IRD 5b-event." This result draws some support from a study of a sea core retrieved from the Faroe Islands that indicated a southward expansion of cold polar waters and drift ice into the North Atlantic at that time (Rasmussen and Thomsen, 2010) (26), which facilitated the deposition of IRD. A diatom-based calibration model established for northern Fennoscandia suggested reduced summer temperatures at 7.2 cal ka BP (Korhola and Weckström, 2000; Fig. 4g) (27). The same cooling event is displayed in sediment from Lake Sumink in northern Poland, where geochemical and pollen data indicate a summer temperature decline between 7.6 and 7.5 cal ka BP (Pędziszewska et al., 2015). The occurrence of extended cold conditions may explain advances in mountain glaciers in Scandinavia centered roughly at 7.3 cal ka BP (Karlén, 1988; Nesje, 2009). Several lakes have been studied farther south, on the Swiss Plateau. Pollen data from Lake Lago Basso indicated a timberline depression between 7.5 and 7.2 cal ka BP caused by poor summertime growing conditions (Haas et al., 1998). The geomorphologic evidence of lake-level change from Lake Seedorf indicated a major rise in lake level. Increased precipitation and reduced summer temperatures producing low evaporation may have been important in the lake-level changes. A similar reduction of the summer temperature was inferred from glacial advances in the Eastern Alps (Nicolussi and Patzelt, 2006; Figure 4d) and in the Austrian Alps, which Patzelt and Bortenschlager (1973) described as the "Frosnitz oscillation." In the Rhone catchment area, a multi-proxy study of a floodplain demonstrated the existence of a long, rapid tripartite climatic change from 7.7 to 7.05 cal ka BP. This rapid change included two phases of abundant hydrology (7.7–7.49 cal ka BP and 7.37–7.05 cal ka BP), between which a short phase of pedogenesis occurred (7.49–7.37 cal ka BP; Berger et al., 2016). A reconstruction of lake-level changes based on 180 radiocarbon, tree-ring, and archaeological dates from 26 lakes indicated a strong lake-level rise in central Europe between 7.5 and 7.0 cal ka BP (Magny, 2004; Fig. 4h). A recent compilation

https://doi.org/10.5194/cp-2019-89
Preprint. Discussion started: 9 August 2019



of 2,000 $^{14}C$- and optically stimulated luminescence-dated flood units from across Europe and North Africa also showed an episode of increased flooding between 7.5 and 7.0 cal ka BP (Benito et al., 2015). Such synchronous changes in lake levels within a region can be assumed to be climatically driven.

Proceeding through the southern Mediterranean, a number of records provide strong evidence of a dry event between 7.5 and 7.0 cal ka BP, as indicated by lower lake levels and other indicators of dry conditions. The records showing a strong signal were from Lago Preola (Preola Lake; Magny et al., 2011), Grotta di Carburangeli (Carburangeli Cave; Frisia et al., 2006), and the Siculo-Tunisian Strait (Desprat et al., 2012). Specifically, the sedimentological analyses from which lake levels can be inferred registered a sharp fall in water level between 7.5 and 7.3 cal ka BP at Lago Preola in southern Sicily, Italy (Magny et al., 2011; Fig. 4m) (28). Approximately 75 km northeast of Lago Preola, Holocene climate reconstructions have been made from Grotta di Carburangeli, where low $\delta^{13}C$ and $\delta^{18}O$ excursions from a U/Th-dated stalagmite pointed to cold and dry climate conditions at approximately 7.5 cal ka BP (Frisia et al., 2006). A marine pollen record from a core from the Siculo–Tunisian Strait indicated noticeable changes in the herbaceous composition, in particular strong reductions in Cyperaceae and an increase in Asteraceae as the Mediterranean forest expanded between 7.3 and 7.0 cal ka BP (Desprat et al., 2013) (29). In contrast, clear proxy evidence of increased moisture was apparent in records from the northern Mediterranean. These included evidence from Lake Accesa (Magny et al., 2007), Lake Ledro (Magny et al., 2012), and the South Adriatic Sea (Siani et al., 2013). A high-resolution lake-level reconstruction using a range of sedimentological analysis and level indicators showed a highstand around 7.3 cal ka BP at Lake Accesa in Tuscany, north-central Italy (Magny et al., 2007; Fig. 4j) (30). Similarly, in Lake Ledro, a rising water level was recorded during the period of 7.3–7.0 cal ka BP and coincided with a strong expansion of *Abies* (Magny et al., 2012). A record of SST changes derived from the South Adriatic Sea indicated significant cooling between 7.5 and 7.3 cal ka BP, according to an assumed

https://doi.org/10.5194/cp-2019-89
Preprint. Discussion started: 9 August 2019



calibration of planktonic foraminifera and an isotopic paleothermometer (Siani et al., 2013; Fig. 4k) (31). This cooling led to the reactivation of the convective overturn and the formation of sapropel S1b in the Adriatic as well as in nearby deep basins (Tesi et al., 2017).

Several studies have revealed possible imprints of the 7.5 and 7.0 cal ka BP event in the western and eastern Mediterranean. In the western Mediterranean, marine core MD99-2343 from the island of Minorca showed clear evidence of an abrupt near-surface cooling at 7.2 cal ka BP, based on increases in the *G. bulloides* $\delta^{18}O$ (Frigola et al., 2007) (32). A dry interval in core MD95-2043 correlative with this event was indicated by the decreased forest pollen percentages (Fletcher et al., 2012) (33). A similar decrease in percentages of evergreen tree pollen around 7.5 cal ka BP was recorded in sediment from Padul Lake in Andalucía, Spain, suggesting a cold and dry climate (Ramos-Román et al., 2018; Fig. 4c) (34). These pollen records closely match a high-resolution alkenone-based quantitative temperature reconstruction from the Alboran Sea, which revealed a 1 °C cooling at approximately 7.3 cal ka BP, stated to be mean-annual (Rodrigo-Gámiz et al., 2014). In the eastern Mediterranean, a multi-proxy composite record with a 7-year resolution from Jeita Cave in Lebanon revealed wetter climate conditions between 7.4 and 7.1 cal ka BP, a period characterized by relatively negative $\delta^{13}C$ and $\delta^{18}O$ values (Cheng et al., 2015; Fig. 4i) (36). Wet conditions are also supported by an increase in the stalagmite growth rate evidenced by high Sr/Ca ratios. However, a trend towards more arid conditions after 7.5 cal ka BP was indicated by oxygen-isotopic composition of carbonate from Nar Lake, Turkey (Roberts et al., 2016). The oxygen-isotopic shift to heavier values of a speleothem from Soreq Cave in Israel, which was thought to be a response to a decrease in precipitation, provides additional evidence for a changing climate between 7.5 and 7.2 cal ka BP (Bar-Matthews et al., 1999; Fig. 4l) (35).

Taken with the records from the Mediterranean discussed above, this proxy evidence revealed a contrasting paleohydrological pattern between 7.5 and 7.0 cal ka BP, with drier conditions in the southern Mediterranean and moister conditions in the northern area. This pattern indicating inverse precipitation variability across the Mediterranean was also noted by Magny et al. (2013), who combined lacustrine and marine records from the central Mediterranean along a north–south transect to show clear evidence for wetter conditions to the north of ca. 40 °N and drier conditions to the south between 7.5 and 7.0 cal ka BP.

Overall, most of the high-time-resolution records from Europe and the Mediterranean clearly register the occurrence of the 7.5–7.0 cal ka BP event. In general, it is marked by cooling and increased moisture in north-central Europe and, by contrast, precipitation variability in the Mediterranean, including southern drying and a northern increase in water availability.

https://doi.org/10.5194/cp-2019-89
Preprint. Discussion started: 9 August 2019


Climate of the Past Discussions

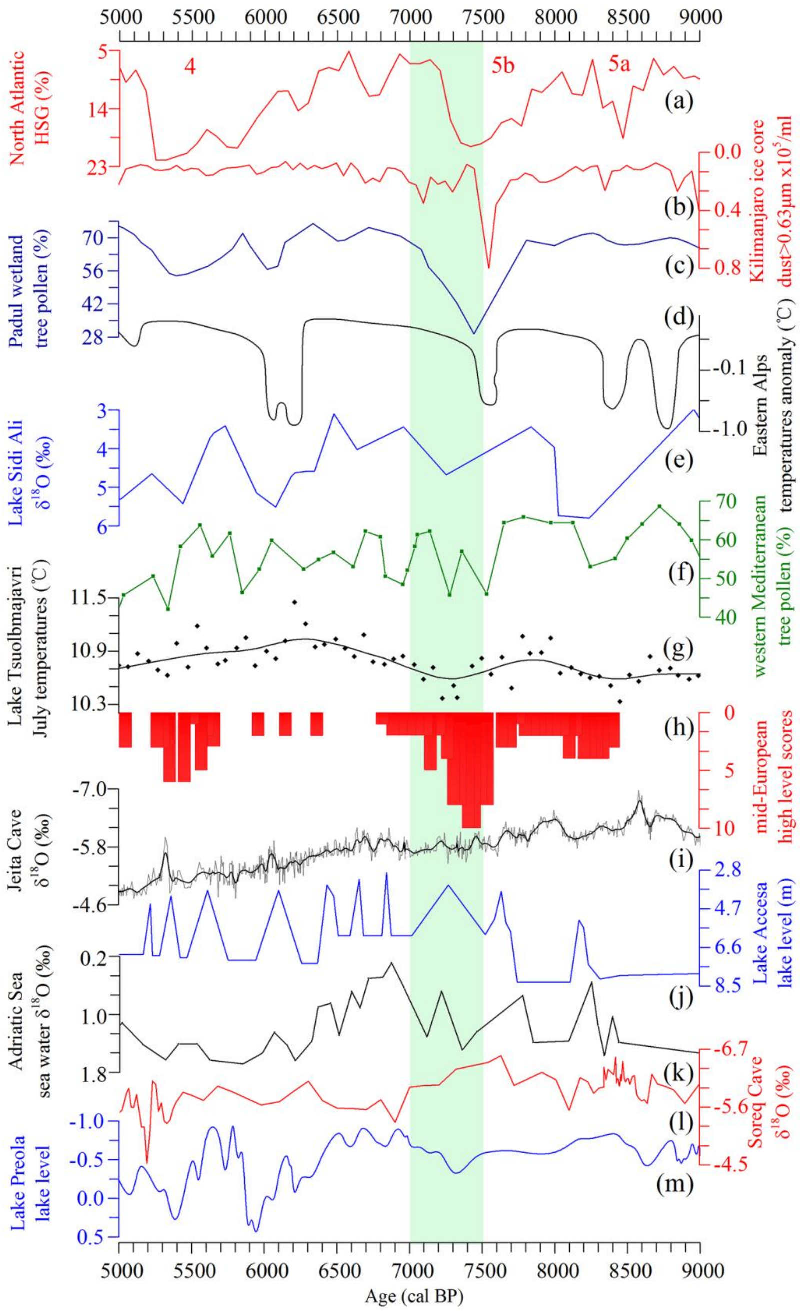


**Figure 4.** Proxy time series for Europe and the Mediterranean. (a) Hematite-stained grains from the North Atlantic (Bond et al., 2001). (b) Dust flux from Mt. Kilimanjaro (Thompson et al., 2002). (c) Mediterranean forest percentages from

https://doi.org/10.5194/cp-2019-89
Preprint. Discussion started: 9 August 2019



Padul Lake. (d) Summer temperature anomalies from the Eastern Alps (Nicolussi and Patzelt, 2006). (e) Ostracod $\delta^{18}O$ from Lake Sidi Ali (Zielhofer et al., 2017a). (f) Tree pollen from the western Mediterranean (Fletcher et al., 2012). (g) Reconstructed mean July temperatures from Lake Tsuolbmajavri. (h) High lake-level scores (number of dates) from mid-Europe (Magny, 2004). (i) Stalagmite $\delta^{18}O$ from Jeita Cave, Lebanon (Cheng et al., 2015). (j) Lake-level reconstruction from Lake Accesa, northern Italy (Magny et al., 2007). (k) Sea water $\delta^{18}O$ from the Adriatic Sea (Siani et al., 2013). (l) Stalagmite $\delta^{18}O$ from Soreq Cave, Israel (Bar-Matthews et al., 1999). (m) Lake-level reconstruction from Lake Preola, southern Italy (Magny et al., 2011).

### 3.4 Africa

A high-resolution, multi-proxy analysis of sediments from the Nile margin indicated a decrease in Nile River contribution and an increase in aeolian Saharan contribution at approximately 7.5 cal ka BP (Revel et al., 2010) (37). Because the Nile discharge is fed by river flow from the Ethiopian Plateau, its reduction is a direct marker of reduced rainfall in the Highlands, likely reflecting restricted southward migration of the Intertropical Convergence Zone. To the west, in the North African Middle Atlas range, proxy studies of lithogenic grain sizes and geochemistry on 26 dates constrained core from Lake Sidi Ali, indicating an enhanced Saharan dust supply into the lake at 7.3 cal ka BP. This does not solely reflect increased aridity, as shown by AMS$^{14}$C, in the Mediterranean of Northwest Africa, but it does imply aridity at a *trans*-Saharan scale (2017b) (38). These proxies display similarities with the stable isotopes of ostracod shells, indicating decreases in western Mediterranean winter rain (Zielhofer et al., 2017a; Fig. 4e). The isotopic and geochemical analyses of core ODP 658C retrieved on the continental slope off Northwest Africa, suggested that large amounts of aeolian dust had been deflated from the Saharan to the eastern Atlantic between 7.5 and 7.0 cal ka BP (Cole et al., 2009). These data were paralleled by a high-altitude ice core record from Mt. Kilimanjaro, which revealed a peak in the aeolian dust precisely dated to 7.5 cal ka BP that was clearly deposited during an extremely arid period (Thompson et al., 2002; Fig. 4b) (39). The proxy information

https://doi.org/10.5194/cp-2019-89
Preprint. Discussion started: 9 August 2019



discussed above suggested that an arid episode from 7.5 to 7.0 cal ka BP occurred midway through a prolonged humid period that began in the early Holocene.

### 3.5 Polar Region

High-time-resolution and high-quality ice core records from the polar region provide compelling evidence for this climate change. The most important result was the occurrence of extreme values in the Greenland Ice Sheet Project 2 (GISP2) $\delta^{18}O$, indicative of an air temperature trough over Greenland during the period of 7.5–7.0 cal ka BP (Stuiver et al., 1995; Fig. 5c) (40). Recently, argon and nitrogen isotopes of trapped air in the GISP2 ice core have been used to reconstruct past temperatures at GISP2 and have indicated colder climate conditions (Kobashi et al., 2017; Fig. 5b). Evidence also exists for colder temperatures in Antarctica, as evidenced by $\delta^{18}O$ values in the Taylor Dome (Steig et al., 2000; Fig. 5a) (41). Dust-size records in two ice cores derived from East Antarctica revealed pronounced changes in atmospheric circulation (Delmonte et al., 2005). Furthermore, signs of anomalies in other regions are often indicated in the polar ice core records. For example, sharp anomalies in major ion concentrations from the GISP2 ice core demonstrated a considerable change in atmospheric circulation at that time. Among these anomalies were increased levels of $Na^+$, $K^+$, and $Ca^{2+}$, which are caused by an expansion of the northern polar vortex, strengthening of the Siberian high, and intensification of the northern westerlies, resulting in increased atmospheric loading of aerosols from dust sources over the ice sheet (Mayewski et al., 1997). A proxy for the wetland extent, the $CH_4$ concentration record derived from Greenland Ice Core Project (GRIP) ice core, visually showed a reduction indicative of increased aridity of the tropical area between 7.4 and 7.3 cal ka BP (Blunier et al., 1995; Fig. 5g) (42). These ice core records showed that conditions changed synchronously in the polar region and far from it, demonstrating that a widespread event did occur.

https://doi.org/10.5194/cp-2019-89
Preprint. Discussion started: 9 August 2019

Climate of the Past
Discussions

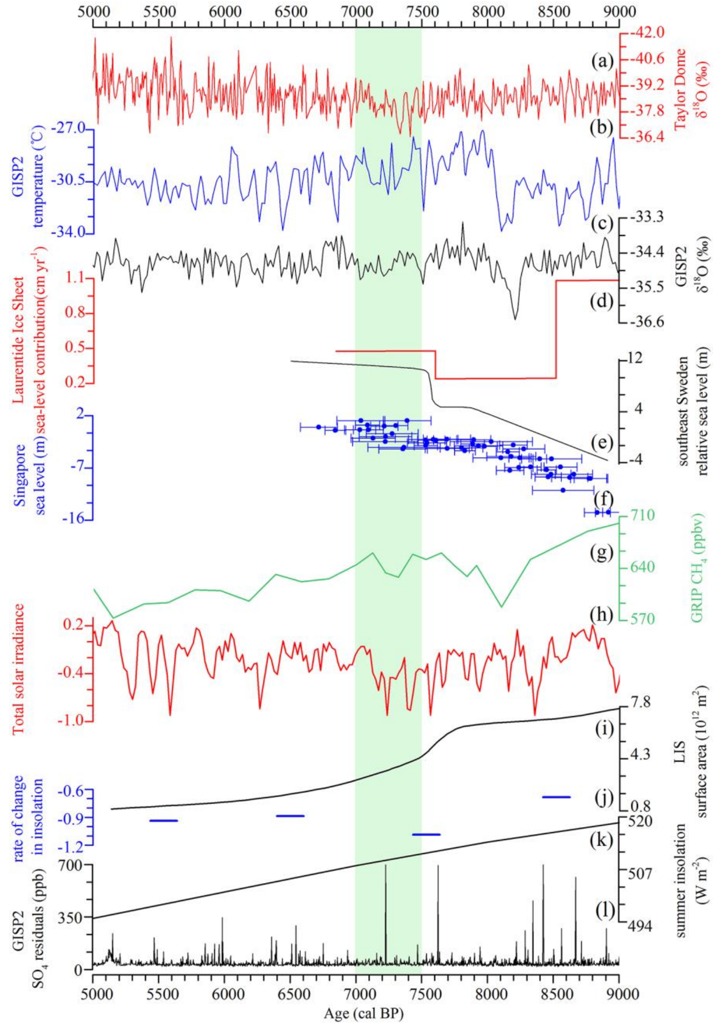


**Figure 5.** Proxy time series for ice core and climate-forcing series. (a) $\delta^{18}O$ for Taylor Dome (Steig et al., 2000). (b) Reconstructed temperature from argon and nitrogen isotopes for the Greenland Ice Sheet Project 2 (GISP2) ice core (Kobashi et al., 2017). (c) $\delta^{18}O$ for GISP2 ice core (20-year resolution; Stuiver et al., 1995). (d) The Laurentide Ice Sheet sea-level contribution (Carlson et al., 2008). (e) Sea-level reconstruction for Singapore (Bird et al., 2007). (f) Sea-level reconstruction for southeast Sweden. (g) $CH_4$ for the Greenland Ice Core Project (GRIP; Blunier et al., 1995). (h) Total solar irradiance based on $^{10}Be$ $^{14}C$ in tree rings and polar ice cores

https://doi.org/10.5194/cp-2019-89
Preprint. Discussion started: 9 August 2019



(Steinhilber et al., 2012). (i) The Laurentide Ice Sheet area (Dyke et al., 2003). (j) The rate of change in annual insolation (Zhao et al., 2010). (k) Summer insolation at 60 °N (Berger and Loutre, 1991). (l) $SO_4$ residuals for the GISP2 (Zielinski et al., 1996).

### 3.6 Sea Level

The complex patterns of hydrological changes and the global temperature cooling appear to be consistent with a rapid sea-level rise around the world between 7.5 and 7.0 cal ka BP. A high-resolution sea-level record, through systematically dating the lacustrine-to-marine and marine-to-lacustrine transitions, was derived from the southeastern Swedish Baltic coast. A rapid sea-level rise of ~4.5 m indicated by nearly synchronous flooding was dated to 7.6 cal ka BP (Yu et al., 2007; Fig. 5e) (43). This rapid sea-level rise was not restricted to high latitude and a similar sea-level rise was identified in other regions remote from the ice-loading effects. Of particular significance to the present study is detailed mapping of the internal structure of the Yellow River delta and its submarine Holocene equivalents. This result indicted a rapid sea-level rise of 2–3 m at approximately 7.0 cal ka BP that pushed the shoreline 200 km westward (Liu et al., 2004) (44). Farther south, pollen, algal, fungal spore, and microcharcoal data from the Neolithic Kuahuqiao site in the Lower Yangtze region indicated a rapid sea-level rise at 7.5 cal ka BP, inducing a marine transgression that inundated the site region, leading to the stoppage of early rice cultivation and abandonment of the site (Zong et al., 2007) (45). This hypothesis seemed to be confirmed by a recent study from the same area, which used a rich data set of radiocarbon dates to reveal a sea-level rise of 2 m from 7.4 to 7.2 cal ka BP (Wang et al., 2012). In Singapore, the combination of a high-resolution sea-level curve derived from 50 dates representing different sea-level index points with the sedimentation rate, organic $\delta^{13}C$, and foraminiferal $\delta^{13}C$ indicated a sea-level rise of 3–5 m from 7.5 to 7.0 cal ka BP (Bird et al., 2007, 2010; Fig. 5f) (46). In the Caribbean–Atlantic region, a study of the elevations and ages of drowned *Acropora palmata* reefs from the Grand Cayman documented a catastrophic, meter-scale

https://doi.org/10.5194/cp-2019-89
Preprint. Discussion started: 9 August 2019



sea-level rise dated to 7.6 cal ka BP (Blanchon and Shaw, 1995; Blanchon et al., 2002) (47).

A rapid rise in sea level between 7.5 and 7.0 cal ka BP can be found from the southeastern Swedish Baltic coast, the Yellow River delta, the Yangtze delta, Singapore, and into the Caribbean Sea, suggesting that it is global in extent. Several authors have suggested that it can be attributed to a sudden increase in ocean mass (Yu et al., 2007; Bird et al., 2010), most likely caused by the final decay of the Labrador sector of the Laurentide Ice Sheet at that time (Dyke et al., 2003; Fig. 5i). This explanation is supported by geologic evidence from the Labrador Sea that suggests an accelerated Laurentide Ice Sheet retreat between 7.6 and 7.0 cal ka BP (Carlson et al., 2008; Fig. 5d).

## 4 Discussion

The combination of sea-level data with different types of paleoclimate proxies from Asia, the Americas, Europe and the Mediterranean, Africa, and the polar region reveals a pronounced climate anomaly between 7.5 and 7.0 cal ka BP. In the Asian monsoon domain, high-time-resolution speleothem $\delta^{18}O$ records and lacustrine proxy records show a summer monsoon reduction that is synchronous with a decline in temperature (Neff et al., 2001; Yu et al., 2004; Wang et al., 2005; An et al., 2012; Cai et al., 2012). In Africa, proxy records show clear indications of a dry interval, as evidenced by a low Nile discharge and increased aeolian flux on the Atlantic coast of the Western Sahara and in the Kilimanjaro ice core (Thompson et al., 2002; Revel et al., 2010; Zielhofer et al., 2017a). Conversely, in the South American monsoon region, speleothem $\delta^{18}O$ records with a high time resolution suggest an intensification of monsoon precipitation (Str ƙis et al., 2011; Bernal et al., 2016). In western North America, cold–wet climate conditions were evident in an SST record and in two speleothem $\delta^{18}O$ records, one of which comes from the North American monsoon region (Asmerom et al., 2007; Marchitto et al., 2010; Ersek et al., 2012). Changes in the amount of rainfall seen in proxy records from the several monsoon domains were the manifestation of a southward migration of the Intertropical Convergence Zone,

https://doi.org/10.5194/cp-2019-89
Preprint. Discussion started: 9 August 2019



with the exception of a speleothem $\delta^{18}O$ record from the Pink Panther Cave from the North American monsoon region. In north-central Europe, an IRD spike (Bond et al., 2001), widespread mountain glacial advances (Karlén, 1988), and higher lake levels (Magny, 2004) pointed to cold–wet climate conditions. In the Mediterranean, a number of proxy records provide evidence for a climate pattern of drier conditions in the southern Mediterranean and moister conditions over the northern area (Magny et al., 2013). A pattern of opposing hydrological variability is apparent between the northern and southern latitudes of the eastern North Atlantic region, potentially linked to enhanced westerlies. In the polar region, ice core records reveal intensified atmospheric circulation and generally lower temperatures (Stuiver et al., 1995; Mayewski et al., 1997). These climate anomalies are also synchronous with a rapid sea-level rise recorded from the tropics to the northern high-latitude regions (Yu et al., 2007; Zong et al., 2007; Bird et al., 2010).

We should stress that the strength of the climate signal varies from being relatively complacent to dramatic, such as a summertime cooling of 2 °C that led to a fundamental vegetation shift within the Daihai Lake catchment, whereas overcooling of SSTs to below 18 °C resulted in at least nine abrupt massive mortality events in reef corals. Our comparison among records also indicates inconsistencies in the timing of the 7.5–7.0 cal ka BP event, but one should be cautious in ascribing too much significance to these age differences, bearing in mind that observing a close correspondence in time can be difficult for possible anomalous events that often last only a few centuries across many proxy records from widely separate places. This difficulty is due in part to the different types of paleoclimate proxy records having resolutions ranging from several decades to several centuries in length and each individual proxy record also containing dating uncertainties. Overall, differences in climate from region to region and differences in the sensitivity of the climate proxies from record to record may explain why the signs, intensities, and times of this climate change can vary across different areas. We can thus still assert that the globally distributed signatures for a climate event from 7.5–7.0 cal ka BP are sufficient to demonstrate changes worldwide and large enough to have significant effects on ecosystems.

We must also consider why the 7.5–7.0 cal ka BP event has received relatively little attention compared with other Holocene climate events. First, the 7.5–7.0 cal ka BP occurs close in time to an 8.2 cal ka BP event. Fluctuations in proxy records occurring around that time may be due to the effects of the terminating 8.2 cal ka BP event because of the relatively imprecise dating of early Holocene proxy data. Second, the magnitude of environmental and climatic change around 7.5–7.0 cal ka BP was small and not easily observed in the geological record. Because the 7.5–7.0 cal ka BP event occurred during the Holocene Climate Maximum, the relatively high precipitation and temperature of this period would offset the cooling and drying impact of the event. Third, not all the oscillations that apparently took place are visible in each of the available records, which may be because many records lack a sufficiently high time resolution and precise dating.

**5 Possible Causes for the 7.5–7.0 cal ka BP Event**

Four main factors have been invoked to explain the climate changes at 7.5–7.0 cal ka BP: orbital forcing, solar activity, volcanic eruption, and meltwater flux. Changes in insolation have been considered a major control on climate changes on orbital timescales (Berger and Loutre, 1991; Wang et al., 2005). A prominent example of this control occurred during the early to mid-Holocene when higher than present Northern Hemisphere summer insolation rendered the North African monsoon strong enough to turn the Sahara Desert into a green and verdant landscape (deMenocal et al., 2000). High-resolution and absolute-dated speleothem $\delta^{18}O$ records from the Asian monsoon domain and the South American monsoon domain also indicate that long-term histories of summer monsoon intensity are associated with summer insolation (Fleitmann et al., 2003; Wang et al., 2005; Bernal et al., 2016). As indicated in Figure 5k, the 7.5–7.0 cal ka BP event occurs within the general context of gradually decreasing Northern Hemisphere summer insolation (Berger and Loutre, 1991). Consistent with this insolation change, the beginning of a long-term climate reversal toward cooling was recorded after 7.5 cal ka BP, according to a reconstruction of global temperature from 73 globally distributed records (Marcott et al., 2013). Similarly, pollen records from the western Mediterranean indicate a long-term decline in forest levels from 7.5 cal ka BP, which paralleled the decrease in Northern Hemisphere summer insolation (Fletcher et al., 2012). An abrupt and nonreversing increase in Guliya ice core $\delta^{18}O$ values after 7.5 cal ka BP provides an example of the rapid transition from warmer conditions to cooler conditions (Thompson et al., 1989). However, progressive insolation changes alone are not likely to render such an abrupt climate change at 7.5–7.0 cal ka BP. Instead, we can turn to general circulation models, which have shown that subtle changes in insolation, aided by positive feedback from the atmosphere, ocean, sea ice, and vegetation, could produce significant climate shifts owing to the nonlinear reaction of the climate system (deMenocal et al., 2000). Furthermore, the fastest rate of annual insolation decline during the 7.5–7.0 cal ka BP event could have promoted a more unstable climate through rapidly changing thermal gradients at different latitudes (Zhao et al., 2010; Fig. 5j).

The period of 7.5–7.0 cal ka BP is characterized by a series of negative total solar irradiance anomalies, generally larger than any others in the Holocene (Steinhilber et al., 2012; Fig. 5h). The most obvious mechanism for a solar influence on the climate involves the direct effect of the observed variation in total solar irradiance for heating the Earth system (Gray et al., 2010). Model studies (Haigh, 1996) imply that at times of reduced solar irradiance, the relatively large reduction in incoming ultraviolet radiation causes decreases in lower stratospheric ozone formation, thus cooling this layer differentially with respect to latitude. These changes in stratospheric ozone induce a dramatic reorganization of tropospheric circulation patterns, such as the contraction of the Hadley circulation, the weakening of the Walker circulation, and a positive North Atlantic Oscillation-type circulation. The solar minimum also involves less heating of cloud-free areas of the subtropics, evaporating less moisture (Meehl et al., 2009). Thus, less moisture is carried by the

https://doi.org/10.5194/cp-2019-89
Preprint. Discussion started: 9 August 2019



trade winds to the convergence zones, where it fuels intensification of the Hadley and Walker circulations. The two mechanisms act together to result in a southward migration of the Intertropical Convergence Zone, an increasingly El Niño-like state, and a strong increase in the westerly flow, generating global climate variability on centennial to millennial timescales (Haigh, 1996). The close correspondence in times of solar irradiance minima, cooler sea surface temperatures in the Soledad Basin (Marchitto et al., 2010), a positive speleothem $\delta^{18}O$ value in the Asian monsoon domain (Neff et al., 2001; Gupta et al., 2005; Wang et al., 2005; Cai et al., 2012), and a negative speleothem $\delta^{18}O$ value in the South America monsoon region (Bernal et al., 2016) confirm the proposed relationship between solar forcing and climate change. It is important to point out that a southward migration of the Intertropical Convergence Zone cannot account for wet conditions in the North American monsoon region during 7.5–7.0 cal ka BP, as implied by the speleothem $\delta^{18}O$ records from the Pink Panther Cave in the southwestern United States. Asmerom et al. (2007) have suggested that climate change in western North America may have had a complex regional pattern and that a teleconnected Pacific response to solar forcing could be responsible. A correlation discovered between nuclide production rates ($^{14}C$ and $^{10}Be$) and drift ice deposition recorded in North Atlantic sediments led to the suggestion that a significant part of the centennial- to millennial-scale climate variability during the Holocene was driven by solar forcing (Bond et al., 2001; Renssen et al., 2006). Goosse et al. (2002) have suggested that variations in solar irradiance may trigger a reduction in North Atlantic Deep Water production quite similar in the magnitude, duration, and spatial pattern of climate anomalies to those due to freshwater forcing. The reductions in North Atlantic Deep Water production may have been an amplifying mechanism that could contribute to transmitting solar signals globally. Although the potential transmission mechanisms are unclear, atmospheric teleconnections in transferring climate variability from the North Atlantic to the global scope are the best candidate (Haug et al., 2001; Zhang and Delworth, 2005; Liu et al., 2013). Evidence that the interval of increased IRD in the North Atlantic

https://doi.org/10.5194/cp-2019-89
Preprint. Discussion started: 9 August 2019



(Bond et al., 2001) corresponds to these episodes of cooler SSTs in the Soledad Basin (Marchitto et al., 2010), increased sea surface salinity in the Florida Straits (Schmidt et al., 2012), strong lake-level rise in central Europe (Magny, 2004), positive speleothem $\delta^{18}O$ values in the Asian monsoon domain (Neff et al., 2001; Gupta et al., 2005; Wang et al., 2005; Cai et al., 2012), a negative speleothem $\delta^{18}O$ value in the South American monsoon region (Stríkis et al., 2011), and decreased winter precipitation in northwest Africa (Zielhofer et al., 2017a) confirms a strong coupling between North Atlantic cooling and the global climate.

Another possible external forcing responsible for sharp anomalies between 7.5 and 7.0 cal ka BP is volcanic eruption. Large volcanic eruptions are well known to inject sulfur dioxide into the lower stratosphere, which forms aerosol particles that affect both shortwave and longwave radiation (Zielinski et al., 1996; Robock, 2000). This disturbance to the radiation balance affects surface temperatures through direct radiative effects as well as through indirect effects on the atmospheric circulation (Robock, 2000). Studies show significant continental-scale summer cooling over Europe in response to changes in circulation beginning in the volcanic eruption year and persisting for 1–2 more years (Fischer et al., 2007). Coincident with the timing of the climate shift of the 7.5–7.0 cal ka BP event was the large eruption of Mount Mazama, which deposited ash in GISP2 ice core precisely dated to 7,627 ± 150 cal BP. Zdanowicz et al. (1999) suggested that the eruption led to a total stratospheric aerosol loading of between 88 and 224 Mt and produced a temperature depression of ~0.6 to 0.7 °C at mid to high northern latitudes for 1–3 yr. In addition to temperature changes, studies suggest that precipitation apparently changes after large volcanic eruptions because a positive phase of the North Atlantic Oscillation induces stronger westerlies (Fischer et al., 2007) and hemisphere temperature contrasts, resulting in the southward migration of the Intertropical Convergence Zone (Ridley et al., 2015). However, a lasting influence on the regional climate conflicts with the short residence time of stratospheric sulfate aerosols from a single eruption. Recent climate model simulations have indicated that a single large volcanic eruption could induce rapid

https://doi.org/10.5194/cp-2019-89
Preprint. Discussion started: 9 August 2019




atmospheric and ocean surface cooling for approximately 16 yr and that lower temperatures could persist at high northern latitudes for even a century or longer owing to sea ice and ocean feedback (Miller et al., 2012; Kobashi et al., 2017). The interval of 7.5–7.0 cal ka BP features multiple large volcanic eruptions (http://volcano.si.edu/volcano.cfm?vn=283001; Fig. 5m) that could have caused the global average summer cooling, a weakened Afro-Asian monsoon circulation, and strengthened westerlies, in agreement with proxy records indicating a low-latitude precipitation reduction and wet conditions over north-central Europe (Robock, 2000; Fischer et al., 2007; Man et al., 2014).

Carlson et al. (2007) used a rich data set of radiocarbon dates and $^{10}$Be ages to infer a retreat of the Laurentide Ice Sheet between 7.5 and 7.0 cal ka BP. This recession led to the formation of numerous glacial lakes, which drained in approximately 16 meltwater pulses with fluxes exceeding 0.015 Sv into the Labrador Sea, Ungava Bay, and Hudson Bay (Jansson and Kleman, 2004). The global sea-level rise indicated by proxy records demonstrates frequent meltwater discharge and a sudden increase in ocean mass (Liu et al., 2004; Yu et al., 2007; Bird et al., 2010; Wang et al., 2012). The increased outflow of low-salinity water from the Black Sea into the Northern Aegean between 7.5 and 7.0 cal ka BP caused by the rapid sea-level rises reconnected the Black Sea with the global ocean, providing indirect proof of the recession of the Laurentide Ice Sheet (Herrle et al., 2018). An abrupt drowning of the Black Sea shelf and simultaneous submergence of 100,000 km$^2$ of the continental shelf was also relevant (Ryan et al., 1997). Such a massive freshwater release influences sea water salinity and density, which suppresses North Atlantic deep-water convection and slows the Atlantic Meridional Overturning Circulation (AMOC; Törnqvist and Hijma, 2012). In a core from the continental slope off northeastern Brazil (4°S, 36°W, at a water depth of 2,632 m), Arz et al. (2001) examined Ca intensities and the degree of preservation of the aragonitic shells of *Limacina inflata*, which are linked to the bottom-water corrosiveness, to infer a short-lived weakening of Atlantic thermohaline circulation between 7.5 and 7.0 cal ka BP (Bakker et al.,

https://doi.org/10.5194/cp-2019-89
Preprint. Discussion started: 9 August 2019



2017). The universal climate anomaly modeled in response to the reduced AMOC is the cooling over the North Atlantic, which results in an increased latitudinal temperature gradient in favor of the development of stronger westerly winds (Davis and Brewer, 2009). Strong westerlies would result in a northward shift of Atlantic storm tracks and higher precipitation over the northern latitudes of the eastern North Atlantic region, in contrast to reduced moisture penetration into the southern region (Fletcher et al., 2012; Magny et al., 2013). Convincing support for this interpretation is found in plentiful proxy records indicating a pattern of opposing precipitation variability, with dry conditions in the southwestern Mediterranean (Magny et al., 2011; Desprat et al., 2012; Fletcher et al., 2012) and wetter conditions over north-central Europe and in the northern Mediterranean between 7.5 and 7.0 cal ka BP (Haas et al., 1998; Magny, 2004; Magny et al., 2007). Other climate changes modeled include a southward shift of the Intertropical Convergence Zone (Marshall et al., 2014), a weakening of monsoonal rainfall in Africa and Asia (Zhang and Delworth, 2005; Sun et al., 2011), and cooler temperatures throughout much of the northern hemisphere. This model response has much in common with the reconstructed anomalies from our synthesized paleoclimate data (Magny, 2004; Gupta et al., 2005; Wang et al., 2005; Marchitto et al., 2010; Str ķis et al., 2011; Schmidt et al., 2012; Zielhofer et al., 2017a), suggesting that the reduction of the AMOC probably played a key role in driving global climate change at that time.

It is apparent that a southward migration of the Intertropical Convergence Zone, a reinforcement of the westerlies, and a slowing of the AMOC developed between 7.5 and 7.0 cal ka BP as a consequence of changes in solar activity, volcanic activity, ice sheet dynamics, and summer insolation. These climate modes could explain the most robust features of the 7.5–7.0 cal ka BP climate event in most reconstructions. Determining the relative weighting of such forcings is a desirable research goal.

## 6 Conclusions

From 47 paleoclimatic records from a variety of paleo-archives, including lake sediment, speleothem, marine sediment, and ice core, we have identified a prominent

https://doi.org/10.5194/cp-2019-89
Preprint. Discussion started: 9 August 2019


climate event at 7.5–7.0 cal ka BP. As revealed by our synthesis results, proxy evidence clearly shows that the 7.5–7.0 cal ka BP event is characterized by a weaker Asian summer monsoon and, in comparison, a stronger South American summer monsoon. The event also involves strong cooling and wetter conditions in north-central Europe and in western North America, widespread drying across Africa, and contrasting patterns of precipitation variability throughout the Mediterranean. Strong signals from polar ice core records reveal intensified atmospheric circulation and generally reduced temperatures. At approximately the same time, a rapid sea-level rise occurred on a near-global scale. Despite varying climatic responses in different regions, a globally distributed signature for this event demonstrates that it is of worldwide significance.

These climate signals reflect a southward migration of the Intertropical Convergence Zone, a reinforcement of the westerlies, and a slowing of the AMOC. Changes in climate modes between 7.5 and 7.0 cal ka BP, which could have arisen because of the atmosphere–ocean–land feedback in response to an orbitally induced decrease in solar insolation, large volcanic eruptions, a reduction in solar activity, and meltwater flux into the North Atlantic, induced climate anomalies much like those suggested by the proxy records. The close correspondence in time of the climate anomalies and the forcings suggest that the 7.5–7.0 cal ka BP event was likely caused by a combination of orbital forcing, deglaciation, volcanic eruptions, and solar activity.

This review is in an early stage and gives only a robust analysis of the 7.5–7.0 cal ka BP event. As we have shown, the climate responses are rarely spatially uniform, and it remains exceedingly difficult to draw anomaly maps. Uncertainties remain concerning the spatial dimensions, duration, and magnitude of the climate event. It is also important to develop significantly more research into assessments of potential transmission mechanisms that induce climate change and potential enhancements of natural feedback that may amplify the relatively weak forcing related to fluctuations in solar output and volcanic eruptions. Future advances will require more quantitative or semiquantitative reconstructions and higher resolution records sampled at a higher spatial density to determine, with greater precision, the complexity of the climate response. A better understanding of this event will help in unraveling the underlying climate dynamics and enhance our predictions regarding the likelihood of future rapid climate change and its associated societal impacts.

**Data availability.** The paper is a review and all the data have been collected from previous publications either on an open database or by digitizing figures with GetData2.20 software. In any case, they have been organized in a series of *.xls files, which can be obtained by request to MH.

**Author contributions.** MH and WW conceived the manuscript and wrote most of the manuscript. CDJ contributed to the construction and writing of Sect 1; YZ, ZZ and HH collected data. HZ and QG provided support on the interpretation and gave comments and agreement during the writing process. All the co-authors participated in sharing the data and contributed to the scientific discussion.

**Competing interests**. The authors declare that they have no conflict of interest.

**Acknowledgements.** This work was jointly supported by the National Natural Science Foundation of China (Grant No. 41672176), the Strategic Priority Research Program of Chinese Academy of Sciences, Pan-Third Pole Environment Study for a Green Silk Road (Pan-TPE) (Grant No. XDA20040201), and the National Natural Science Foundation of China (Grant No. 41888101).

## References

1. Alley, R. B. and Ágústsdóttir, A. M.: The 8 k event: Cause and consequences of a major Holocene abrupt climate change, Quaternary Sci. Rev., 24, 1123–1149, 2005.

https://doi.org/10.5194/cp-2019-89
Preprint. Discussion started: 9 August 2019



2. Alley, R. B., Mayewski, P. A., Sowers, T., Stuiver, M., Taylor, K. C., and Clark, P. U.: Holocene climatic instability: A prominent, widespread event 8200 yr ago, Geology, 25, 483–486, 1997.
3. An, Z., Colman, S. M., Zhou, W., Li, X., Brown, E. T., Timothy Jull, A. J., Cai, Y., Huang, Y., Xuefeng Lu, Chang, H., Song, Y., Sun, Y., Xu, H., Liu, W., Jin, Z., Liu, X., Cheng, P., Liu, Y., Ai, L., Li, X., Liu, X., Yan, L., Shi, Z., Wang, X., Wu, F., Qiang, X., Dong, J., Lu, F., and Xu, X.: Interplay between the Westerlies and Asian monsoon recorded in Lake Qinghai sediments since 32 ka, Sci. Rep., 2, 619, 2012.
4. Arz, H. W., Gerhardt, S., Pätzold, J., and Röhl, U.: Millennial-scale changes of surface- and deep-water flow in the western tropical Atlantic linked to Northern Hemisphere high-latitude climate during the Holocene, Geology, 29, 239–242, 2001.
5. Asmerom, Y., Polyak, V., Burns, S., and Rassmussen, J.: Solar forcing of Holocene climate: New insights from a speleothem record, southwestern United States, Geology, 35, 1–4, 2007.
6. Aubán, J. B., Puchol, O. G., Barton, M., McClure, S., and Gordó, S. P.: Radiocarbon dates, climatic events, and social dynamics during the Early Neolithic in Mediterranean Iberia, Quaternary International, 403, 201–210, 2016.
7. Baker, P. A., Fritz, S. C., Garland, J., and Ekdahl, E.: Holocene hydrologic variation at Lake Titicaca, Bolivia/Peru, and its relationship to North Atlantic climate variation, J. Quaternary Sci., 7–8, 655–662, 2005.
8. Bakker, P., Clark, P. U., Golledge, N. R., Schmittner, A., and Weber, M. E.: Centennial-scale Holocene climate variations amplified by Antarctic Ice Sheet discharge, Nature, 541, 72–76, 2017.
9. Bar-Matthews, M., Ayalon, A., Kaufman, A., and Wasserburg, G. J.: The Eastern Mediterranean paleoclimate as a reflection of regional events: Soreq cave, Israel, Earth Planet. Sc. Lett., 166, 85–95, 1999.
10. Benito, G., Macklin, M. G., Panin, A., Rossato, S., Fontana, A., Jones, A. F.,

https://doi.org/10.5194/cp-2019-89
Preprint. Discussion started: 9 August 2019



Machado, M. J., Matlakhova, E., Mozzi, P., and Zielhofer, C.: Recurring flood distribution patterns related to short-term Holocene climatic variability, Sci. Rep., 5, 16398, 2015.

11. Berger, A. and Loutre, M. F.: Insolation values for the climate of the last 10 million years, Quaternary Sci. Rev., 10, 297–317, 1991.
12. Berger, J. F., Delhon, C., Magnin, F., Bonté, S., Peyric, D., Thiébault, S., Guilbert, R., and Beeching, A.: A fluvial record of the mid-Holocene rapid climatic changes in the middle Rhone valley (Espeluche-Lalo, France) and of their impact on Late Mesolithic and Early Neolithic societies, Quaternary Sci. Rev., 136, 66–84, 2016.
13. Berkelhammer, M., Sinha, A., Stott, L., Cheng, H., Pausata, F. S. R., and Yoshimura, K.: An abrupt shift in the Indian Monsoon 4000 Years Ago, In: AGU Geophysical Monograph on Climate and Civilization, Geophys. Res. Lett., 198, 75–87, 2012.
14. Bernal, J. P., Cruz, F. W., Stríkis, N. M., Wang, X., Deininger, M., Catunda, M. C. A.,Ortega-Obregón, C., Cheng, H., Edwards, R. L., and Auler, A. S.: High-resolution Holocene South American monsoon history recorded by a speleothem from Botuverá Cave, Brazil, Earth Planet. Sc. Lett., 450, 186–196, 2016.
15. Bird, M. I., Austin, W. E. N., Wurster, C. M., Fifield, L. K., Mojtahid, M., and Sargeant, C.: Punctuated eustatic sea-level rise in the early mid-Holocene, Geology, 38, 803–806, 2010.
16. Bird, M. I., Fifield, L. K., The, T. S., Chang, C. H., Shirlaw, N., and Lambeck, K.: An inflection in the rate of early mid-Holocene eustatic sea-level rise: A new sea-level curve from Singapore, Coast. Shelf Sci., 71, 523–536, 2007.
17. Blunier, T., Chappellaz, J., Schwander, J., Stauffer, B., and Raynaud, D.: Variations in atmospheric methane concentration during the Holocene epoch, Nature, 374, 46–49, 1995.
18. Blanchon, P., Jones, B., and Ford, D. C.: Discovery of a submerged relic reef and

https://doi.org/10.5194/cp-2019-89
Preprint. Discussion started: 9 August 2019




shoreline off Grand Cayman: further support for an early Holocene jump in sea level, Sediment. Geol., 147, 253–270, 2002.

19. Blanchon, P. and Shaw, J.: Reef drowning during the last deglaciation: Evidence for catastrophic sea-level rise and ice-sheet collapse, Geology, 23, 4–8, 1995.
20. Bond, G., Kromer, B., Beer, J., Muscheler, R., Evans, M. N., Showers, W., Hoffmann, S., Lotti-Bond, R., Hajdas, I., and Bonani, G.: Persistent solar influence on North Atlantic climate during the Holocene, Science, 294, 2130–2136, 2001.
21. Brooks, N.: Cultural responses to aridity in the Middle Holocene and increased social complexity, Quaternary Int., 151, 29–49, 2006.
22. Cai, Y., Zhang, H., Cheng, H., An, Z., Edwards, R. L., Wang, X., Tan, L., Liang, F., Wang, J., and Kelly, M.: The Holocene Indian monsoon variability over the southern Tibetan Plateau and its teleconnections, Earth Planet. Sc. Lett., 335–336, 135–144, 2012.
23. Carlson, A. E., Legrande, A. N., Oppo, D. W., Came, R. E., Schmidt, G. A., Anslow, F. S., Licciardi, J. M., and Obbink, E. A.: Rapid early Holocene deglaciation of the Laurentide ice sheet, Nat. Geosci., 1, 620–624, 2008.
24. Cheng, H., Sinha, A., Verheyden, S., Nader, F. H., Li, X. L., Zhang, P. Z., Yin, J. J., Yi, L., Peng, Y. B., Rao, Z. G., Ning, Y. F., and Edwards, R. L.: The climate variability in northern Levant over the past 20,000 years, Geophys. Res. Lett., 42, 8641–8650, 2015.
25. Cole, J. M., Goldstein, S. L., deMenocal, P. B., Hemming, S. R., and Grousset, F. E.: Contrasting compositions of Saharan dust in the eastern Atlantic Ocean during the last deglaciation and African Humid Period, Earth Planet. Sc. Lett., 278, 257–266, 2009.
26. Davis, B. A. S. and Brewer, S.: Orbital forcing and role of the latitudinal insolation/temperature gradient, Clim. Dynam., 32, 143–165, 2009.
27. Delmonte, B., Petit, J. R., Krinner, G., Maggi, V., Jouzel, J., and Udisti, U.: Ice core evidence for secular variability and 200-year dipolar oscillations in

https://doi.org/10.5194/cp-2019-89
Preprint. Discussion started: 9 August 2019


atmospheric circulation over East Antarctica during the Holocene, Clim. Dynam., 24, 641–654, 2005.

28. deMenocal, P., Ortiz, J., Guilderson, T., Adkins, J., Sarnthein, M., Baker, L., and Yarusinsky, M.: Abrupt onset and termination of the African Humid Period: rapid climate responses to gradual insolation forcing, Quaternary Sci. Rev., 19, 347–361, 2000.
29. Desprat, S., Combourieu-Nebout, N., Essallami, L., Sicre, M. A., Dormoy, I., Peyron, O., Roumazeilles, V. B., and Turon, J. L.: Deglacial and Holocene vegetation and climatic changes in the southern Central Mediterranean from a direct land–sea correlation, Clim. Past, 9, 767–787, 2013.
30. Dong, G.: Neolithic cultural evolution and its environmental driving force in Gansu-Qinghai region problems and perspectives, Mar. Geol. Quaternary Geol., 33, 67–75, 2013 (in Chinese).
31. Dyke, A. S., Moore, A., and Robinson, L.: Deglaciation of North America, Tech. Rep. Open File 1574, Geological Survey of Canada, Ottawa, 2003.
32. Ersek, V., Clark, P. U., Mix, A. C., Cheng, H., and Edwards, R. L.: Holocene winter climate variability in mid-latitude western North America, Nat. Commun., 3, 1–8, 2012.
33. Fischer, E. M., Luterbacher, J., Zorita, E., Tett, S. F. B., Casty, C., and Wanner, H.: European climate response to tropical volcanic eruptions over the last half millennium, Geophys. Res. Lett., 34, L05707, 2007.
34. Fleitmann, D., Burns, S. J., Mudelsee, M., Neff, U., Kramers, J., Mangini, A., and Matter, A.: Holocene forcing of the Indian Monsoon recorded in a stalagmite from southern Oman, Science, 300, 1737–1739, 2003.
35. Fletcher, W. J., Debret, M., and Goñi, M. F. S.: Mid-Holocene emergence of a lowfrequency millennial oscillation in western Mediterranean climate: Implications for past dynamics of the North Atlantic atmospheric westerlies, Holocene, 23, 153–166, 2012.
36. Frigola, J., Moreno, A., Cacho, I., Canals, M., Sierro, F. J., Flores, J. A., Grimalt,

https://doi.org/10.5194/cp-2019-89
Preprint. Discussion started: 9 August 2019

Climate of the Past
Discussions

J. O., Hodell, D. A., and Curtis, J. H.: Holocene climate variability in the western Mediterranean region from a deepwater sediment record, Paleoceanography, 22, PA2209, 2007.

37. Frisia, S., Borsato, A., Mangini, A., Spötl, C., Madonia, G., and Sauro, U.: Holocene climate variability in Sicily from a discontinuous stalagmite record and the Mesolithic to Neolithic transition, Quaternary Res., 66, 388–400, 2006.

38. Goosse, H., Renseen, H., Selten, F. M., Haarsma, R. J., and Opsteegh, J. D.: Potential causes of abrupt climate events: A numerical study with a three-dimensional climate model, Geophys. Res. Lett., 29, 1860, 2002.

39. Gray, L. J., Beer, J., Geller, M., Haigh, J. D., Lockwood, M., Matthes, K., Cubasch, U., Fleitmann, D., Harrison, G., Hood, L., Luterbacher, J., Meehl, G. A., Shindell, D., van Geel, B., and White, W.: Solar influences on climate, Rev. Geophys., 48, RG4001, 2010.

40. Gronenborn, D.: Climate, crises and the neolithisation of Central Europe between IRD-events 6 and 4, in: The Spread of the Neolithic to Central Europe, edited by: Gronenborn, D. and Petrasch, J., Verlag des Romisch-Germanischen Zentralmuseums, Mainz, 61–80, 2010.

41. Gupta, A. K., Das, M., and Anderson, D. M.: Solar influence on the Indian summer monsoon during the Holocene, Geophys. Res. Lett., 32, L17703, 2005.

42. Haas, J. N., Richoz, I., Tinner, W., and Wick, L.: Synchronous Holocene climatic oscillations recorded on the Swiss Plateau and at timberline in the Alps, Holocene, 8, 301–309, 1998.

43. Haigh, J. D.: The impact of solar variability on climate, Science, 272, 981–984, 1996.

44. Haug, G. H., Hughen, K. A., Sigman, D. M., Peterson, L. C., and Röhl, U.: Southward migration of the Intertropical Convergence Zone through the Holocene, Science, 293, 1304–1308, 2001.

45. Herrle, J. O., Bollmann, J., Gebühr, C., Schulz, H., Sheward, R. M., and Giesenberg, A.: Black Sea outfow response to Holocene meltwater events, Sci.

Rep., 8, 4081, 2018.

46. Huang, X., Meyers, P. A., Jia, C., Zheng, M., Xue, J., Wang, X., and Xie, S.: Paleotemperature variability in central China during the last 13 ka recorded by a novel microbial lipid proxy in the Dajiuhu Peat deposit, Holocene, 23, 1123–1129, 2013.
47. Hughes, P. D. M., Blundell, A., Charman, D. J., Bartlett, S., Daniell, J. R. G., Wojatschke, A., and Chambers, F. M.: An 8500 cal. year multi-proxy climate record from a bog in eastern Newfoundland: contributions of meltwater discharge and solar forcing, Quaternary Sci. Rev., 25, 1208–1227, 2006.
48. Intergovernmental Panel on Climate Change (Eds): Climate change 2013: The physical science basis, Cambridge University Press, Cambridge, England, 2013.
49. Jansson, K. N. and Kleman, J.: Early Holocene glacial lake meltwater injections into the Labrador Sea and Ungava Bay, Paleoceanography, 19, PA1001, 2004.
50. Karlén, W.: Scandinavian glacial and climatic fluctuations during the Holocene, Quaternary Sci. Rev., 7, 199–209, 1988.
51. Kobashi, T., Menviel, L., Thömmes, A. J., Vinther, B. M., Box, J. E., Muscheler, R., Nakaegawa, T., Pfister, P. L., Döring, M., Leuenberger, M., Wanner, H., and Ohmura, A.: Volcanic influence on centennial to millennial Holocene Greenland temperature change, Sci. Rep., 7, 1441, 2017.
52. Korhola, A., Weckström, J., Holmström, L., and Erästö, P.: A Quantitative Holocene Climatic Record from Diatoms in Northern Fennoscandia, Quaternary Res., 54, 284–294, 2000.
53. Liu, D., Wang, Y., Cheng, H., Edwards, R. L., and Kong, X.: Cyclic changes of Asian monsoon intensity during the early mid-Holocene from annually-laminated stalagmites, central China, Quaternary Sci. Rev., 121, 1–10, 2015.
54. Liu, J. P., Milliman, J. D., Gao, S., and Cheng, P.: Holocene development of the Yellow River's subaqueous delta, North Yellow Sea, Mar. Geol., 209, 45–67, 2004.

https://doi.org/10.5194/cp-2019-89
Preprint. Discussion started: 9 August 2019



55. Liu, Y. H., Henderson, G. M., Hu, C. Y., Mason, A. J., Charnley, N., Johnson, K. R., and Xie, S. C.: Links between the East Asian monsoon and North Atlantic climate during the 8,200 year event, Nat. Geosci., 6, 117–120, 2013.
56. Lü, H. and Zhang, J.: Neolithic cultural evolution and Holocene climate change in the Guanzhong Basin, Shanxi, China, Quaternary Sci., 28, 1050–1060, 2008 (in Chinese).
57. Magny, M.: Holocene climate variability as reflected by mid-European lake-level fluctuations and its probable impact on prehistoric human settlements, Quaternary Int., 113, 65–79, 2004.
58. Magny, M., de Beaulieu, J. L., Drescher-Schneider, R., Vannière, B., Walter-Simonnet, A. V., Miras, Y., Millet, L., Bossuet, G., Peyron, O., Brugiapaglia, E., and Leroux, A.: Holocene climate changes in the central Mediterranean as recorded by lake-level fluctuations at Lake Accesa (Tuscany, Italy), Quaternary Sci. Rev., 26, 1736–1758, 2007.
59. Magny, M., Joannin, S., Galop, D., Vannière, B., Haas, J. N., Bassetti, M., Bellintani, P., Scandolari, R., and Desmet, M.: Holocene palaeohydrological changes in the northern Mediterranean borderlands as reflected by the lake-level record of Lake Ledro, northeastern Italy, Quaternary Res., 77, 382–396, 2012.
60. Magny, M., Nebout, N. C., de Beaulieu, J. L., Bout-Roumazeilles, V., Colombaroli, D., Desprat, S., Francke, A., Joannin, S., Ortu, E., Peyron, O., Revel, M., Sadori, L., Siani, G., Sicre, M. A., Samartin, S., Simonneau, A., Tinner, W., Vanniere, B., Wagner, B., Zanchetta, G., Anselmetti, F., Brugiapaglia, E., Chapron, E., Debret, M., Didier, J., Essallami, L., Galop, D., Gilli, A., Kallel, N., Millet, L., Stock, A., Turon, J. L., and Wirth, S.: North-south palaeohydrological contrasts in the central Mediterranean during the Holocene: tentative synthesis and working hypotheses, Clim. Past, 9, 2043–2071, 2013.
61. Magny, M., Vannière, B., Calo, C., Millet, L., Leroux, A., Peyron, O., Zanchetta, G., Mantia, T. L., and Tinner, W.: Holocene hydrological changes in south-western Mediterranean as recorded by lake-level fluctuations at Lago

https://doi.org/10.5194/cp-2019-89
Preprint. Discussion started: 9 August 2019



Preola, a coastal lake in southern Sicily, Italy, Quaternary Sci. Rev., 30, 2459–2475, 2011.

62. Man, W., Zhou, T., and Jungclaus, J. H.: Effects of large volcanic eruptions on global summer climate and East Asian Monsoon changes during the last millennium: analysis of MPI-ESM simulations, J. Climate, 27, 7394–7409, 2014.
63. Marchitto, T. M., Muscheler, R., Ortiz, J. D., Carriquiry, J. D., and van Geen, A.: Dynamical response of the tropical Pacific Ocean to solar forcing during the Early Holocene, Science, 330, 1378–1381, 2010.
64. Marcott, S. A., Shakun, J. D., Clark, P. U., and Mix, A. C.: A reconstruction of regional and global temperature for the past 11,300 years, Science, 339, 1198–1201, 2013.
65. Marshall, J., Donohoe, A., Ferreira, D., and McGee, D.: The ocean's role in setting the mean position of the Inter-Tropical Convergence Zone, Clim. Dynam., 42, 1967–1979, 2014.
66. Mayewski, P. A., Meeker, L. D., Twickler, M. S., Whitlow, S., Yang, Q., Lyons, W. B., and Prentice, M.: Major features and forcing of high-latitude northern hemisphere atmospheric circulation using a 110,000-year-long glaciochemical series, J. Geophys. Res. Ocean., 102, 26345–26366, 1997.
67. Mayewski, P. A., Rohling, E. E., Stager, J. C., Karlén, W., Maasch, K., Meeker, L. D., Meyerson, E. A., Gasse, F., van Kreveld, S., Holmgren, K., Lee-Thorp, J., Rosqvist, G., Rack, F., Staubwasser, M., Schneider, R. R., and Steig, E. J.: Holocene climate variability, Quaternary Res., 62, 243–255, 2004.
68. McManus, J. F., Francois, R., Gherardi, J. M., Keigwin, L. D., and Brown-Leger, S.: Collapse and rapid resumption of Atlantic meridional circulation linked to deglacial climate changes, Nature, 428, 834–837, 2004.
69. Meehl, G. A., Arblaster, J. M., Matthes, K., Sassi, F., and van Loon, H.: Amplifying the Pacific Climate System Response to a Small 11-Year Solar Cycle Forcing, Nature, 325, 1114–1118, 2009.
70. Menounos, B., Osborn, G., Clague, J. J., and Luckman, B. H.: Latest Pleistocene

https://doi.org/10.5194/cp-2019-89
Preprint. Discussion started: 9 August 2019



and Holocene glacier fluctuations in western Canada, Quaternary Sci. Rev., 28, 2049–2074, 2009.

71. Menounos, B., Clague, J. J., Osborn, G., Davis, P. T., Ponce, F., Goehring, B., Maurer, M., Rabassa, J., Coronato, A., and Marr, R.: Latest Pleistocene and Holocene glacier fluctuations in southernmost Tierra del Fuego, Argentina, Quaternary Sci. Rev., 77, 70–79, 2013.
72. Miller, G. H., Geirsdóttir, A., Zhong, Y., Larsen, D. J., Otto-Bliesner, B. L., Holland, M. M., Bailey, D. A., Refsnider, K. A., Lehman, S. J., Southon, J. R., Anderson, C., Björnsson, H., and Thordarson, T.: Abrupt onset of the Little Ice Age triggered by volcanism and sustained by sea-ice/ocean feedbacks, Geophys. Res. Lett., 39, L02708, 2012.
73. Nan, Q., Li, T., Chen, J., Chang, F., Yu, X., Xu, Z., and Pi, Z.: Holocene paleoenvironment changes in the northern Yellow Sea: Evidence from alkenone-derived sea surface temperature, Palaeogeogr. Palaeocl., 483, 83–93, 2017.
74. National Research Council: Abrupt Climate Change: Inevitable Surprises, National Academy Press, Washington, DC, 2002.
75. Neff, U., Burns, S. J., Mangini, A., Fleitmann, D., and Matter, A.: Strong coherence between solar variability and the monsoon in Oman between 9 and 6 kyr ago, Nature, 411, 290–293, 2001.
76. Nesje, A.: Latest Pleistocene and Holocene alpine glacier fluctuations in Scandinavia, Quaternary Sci. Rev., 28, 2119–2136, 2009.
77. Nicolussi, K. and Patzelt, G.: Klimawandel und Veränderungen an der alpinen Waldgrenze-aktuelle Entwicklungen im Vergleich zur Nacheiszeit, BFW Praxisinformationen, 10, 3–5, 2006.
78. Ning, D., Zhang, E., Sun, W., Chang, J., and Shulmeister, J.: Holocene Indian Summer Monsoon variation inferred from geochemical and grain size records from Lake Ximenglongtan, southwestern China, Palaeogeogr. Palaeocl., 487, 260–269, 2017.

79. Patzelt, G. and Bortenschlager, S.: Die neuzeitlichen Gletscherschwankungen in der Venedigergruppe (Hohe Tauern, Ostalpen), Zeitschrift für Geomorphologie N.F. Supplement, 9, 5–57, 1973.
80. Pędziszewska, A., Tylmann, W., Witak, M., Piotrowska, N., Maciejewska, E., and Latałowa, M.: Holocene environmental changes reflected by pollen, diatoms, and geochemistry of annually laminated sediments of Lake Suminko in the Kashubian Lake District (N Poland), Rev. Palaeobot. Palynol., 216, 55–75, 2015.
81. Pérez-Rodríguez, M., Gilfedder, B. S., Hermanns, Y. M., and Biester H.: Solar Output Controls Periodicity in Lake Productivity and Wetness at Southernmost South America, Sci. Rep., 6, 37521, 2016.
82. Ramos-Román, M. J., Jiménez-Moreno, G., Camuera, J., García-Alix, A., Anderson, R. S., Jiménez-Espejo, F. J., Sachse, D., Toney, J. L., Carrión, J. S., Webster, C., and Yanes, Y.: Millennial-scale cyclical environment and climate variability during the Holocene in the western Mediterranean region deduced from a new multiproxy analysis from the Padul record (Sierra Nevada, Spain), Global Planet. Change, 168, 35–53, 2018.
83. Rasmussen, T. L. and Thomsen, E.: Holocene temperature and salinity variability of the Atlantic Water inflow to the Nordic seas, Holocene, 20, 1223–1234, 2010.
84. Renssen, H., Goosse, H., and Muscheler, R.: Coupled climate model simulation of Holocene cooling events: oceanic feedback amplifies solar forcing, Clim. Past, 2, 79–90, 2006.
85. Revel, M., Ducassou, E., Grousset, F. E., Bernasconi, S. M., Migeon, S., Revillon, S., Mascle, J., Murat, A., Zaragosi, S., and Bosch, D.: 100,000 Years of African monsoon variability recorded in sediments of the Nile margin, Quaternary Sci. Rev., 29, 1342–1362, 2010.
86. Ridley, H. E., Asmerom, Y., Baldini1, J. U. L., Breitenbach, S. F. M., Aquino, V. V., Prufer, K. M., Culleton, B. J., Polyak, V., Lechleitner, F. A., Kennett, D. J., Zhang, M., Marwan, N., Macpherson, C. G., Baldini, L. M., Xiao, T., Peterkin, J. L., Awe, J., and Haug, G. H.: Aerosol forcing of the position of the intertropical

https://doi.org/10.5194/cp-2019-89
Preprint. Discussion started: 9 August 2019




convergence zone since AD 1550, Nat. Geosci., 8, 195–200, 2015.

87. Roberts, N., Allcock, S. L., Arnaud, F., Dean, J. R., Eastwood, W. J., Jones, M. D., Leng, M. J., Metcalfe, S. E., Malet, E., Woodbridge, J., and Yiğitbaşıoğlu, H.: A tale of two lakes: a multi-proxy comparison of Lateglacial and Holocene environmental change in Cappadocia, Turkey, J. Quaternary Sci., 31, 348–362, 2016.

88. Roberts, N., Eastwood, W. J., Kuzucuoglu, C., Fiorentino, G., and Caracuta, V.: Climatic, vegetation and cultural change in the eastern Mediterranean during the mid-Holocene environmental transition, Holocene, 21, 147–162, 2011.

89. Robock, A.: Volcanic eruptions and climate, Rev. Geophys., 38, 191–219, 2000.

90. Rodrigo-Gámiz, M., Martínez-Ruiz, F., Rampen, S. W., Schouten, S., and Sinninghe-Damste, J. S.: Sea surface temperature variations in the western Mediterranean Sea over the last 20 kyr: A dual-organic proxy ($U^{K'}_{37}$ and LDI) approach, Paleoceanography, 29, 87–98, 2014.

91. Ryan, W. B. F., Pitman III, W. C., Major, C. O., Shimkus, K., Moskalenko, V., Jones, G. A., Dimitrov, P., Gorür, N., Sakinç, M., and Yüce, H.: An abrupt drowning of the Black Sea shelf, Mar. Geol., 138, 119–126, 1997.

92. Ryder, J. M. and Thomson, B.: Neoglaciation in the southern Coast Mountains of British Columbia: chronology prior to the late Neoglacial maximum. Can. J. Earth Sci., 23, 273–287, 1986.

93. Sánchez, M. C., Espejo, F. J. J., Vallejo, M. D. S., Bao, J. F. G., Carvalho, A. F., Martinez-Ruiz, F., Gamiz, M. R., Flores, J. A., Paytan, A., Sáez, J. A. L., Peña-Chocarro, L., Carrión, J. S., Morales Muñiz, A., Izquierdo, R. E., Cantal, J. A. R., Dean, R. M., Salgueiro, E., Sánchez, R. M. M., De la Rubia de Gracia, J. J., Francisco, M. C. L., Peláez, J. L. V., Rodríguez, L. L., and Bicho, N. F.: The Mesolithic-Neolithic transition in southern Iberia, Quaternary Res., 77, 221–234, 2012.

94. Schmidt, M. W., Weinlein, W. A., Marcantonio, F., and Lynch-Stieglitz, J.: Solar forcing of Florida Straits surface salinity during the early Holocene,

https://doi.org/10.5194/cp-2019-89
Preprint. Discussion started: 9 August 2019



Paleoceanography, 27, PA3204, 2012.

95. Shi, Y., Kong, Z., Wang, S., Tang, L., Wang, F., Yao, T., Zhao, X., Zhang P., and Shi, S.: Climates and environments of Holocene Megathermal maximum in China, Science in China (Series B), 37, 481–493, 1994.

96. Shuman, B.: Patterns, processes, and impacts of abrupt climate change in a warm world: the past 11,700 years, WIREs Clim. Change, 3, 19–43, 2012.

97. Shuman, B. N. and Marsicek, J.: The structure of Holocene climate change in mid-latitude North America, Quaternary Sci. Rev., 141, 38–51, 2016.

98. Siani, W., Magny, M., Paterne, M., Debret, M., and Fontugne, M.: Paleohydrology reconstruction and Holocene climate variability in the South Adriatic Sea, Clim. Past, 9, 499–515, 2013.

99. Steig, E. J., Morse, D. L., Waddington, E. D., Stuiver,, M., Grootes, P. M., Mayewski, P. A., Twickler, M. S., and Whitlow, S. I.: Wisconsinan and Holocene climate history from an ice core at Taylor Dome, Western Ross Embayment, Antarctica, Geografiska Annaler: Series A, Physical Geography, 82, 213–235, 2000.

100. Steinhilber, F., Abreu, J. A., Beer, J., Brunner, I., Christl, M., Fischer, H., Heikkilä, U., Kubik, P. W., Mann, M., McCracken, K. G., Miller, H., Miyahara, H., Oerter, H., and Wilhelms, F.: 9,400 years of cosmic radiation and solar activity from ice cores and tree rings, P. Natl. Acad. Sci. USA, 109, 5967–5971, 2009.

101. Stríkis, N. M., Cruz, F. W., Cheng, H., Karmann, I., Edwards, R. L., Vuille, M., Wang, X., de Paula, M. S., Novello, V. F., and Auler, A. S.: Abrupt variations in South American monsoon rainfall during the Holocene based on a speleothem record from central-eastern Brazil, Geology, 39, 1075–1078, 2011.

102. Stuiver, M., Grootes, P. M., and Braziunas, T. F.: The GISP2 $\delta^{18}O$ climate record of the past 16,500 years and the role of the sun, ocean, and volcanoes. Quaternary Res., 44, 341–354, 1995.

103. Stuiver, M., Reimer, P. J., and Braziunas, T. F.: High-Precision radiocarbon

age calibration for terrestrial and marine samples, Radiocarbon, 40, 1127–1151, 1998.

104. Sun, Y., Clemens, S. C., Morrill, C., Lin, X., Wang, X., and An, Z.: Influence of Atlantic meridional overturning circulation on the East Asian winter monsoon, Nat. Geosci., 5, 46–49, 2011.

105. Tesi, T., Asioli, A., Minisini, D., Maselli, V., Valle, G. D., Gamberi, F., Langone, L., Cattaneo, A., Montagna, P., and Trincardi, F.: Large-scale response of the Eastern Mediterranean thermohaline circulation to African monsoon intensification during sapropel S1 formation, Quaternary Sci. Rev., 159, 139–154, 2017.

106. Thompson, L. G., Mosley-Thompson, E., Davis, M. E., Bolzan, J. F., Dai, J., Klein, L., Yao, T., Wu, X., Xie, Z., and Gundestrup, N.: Holocene-Late Pleistocene climatic ice core records from Qinghai-Tibetan Plateau, Science, 246: 474–477, 1989.

107. Thompson, L. G., Mosley-Thompson, E., Davis, M. E., Henderson, K. A., Brecher, H. H., Zagorodnov, V. S., Mashiotta, T. A., Lin, P. N., Mikhalenko, V. N., Hardy, D. R., and Beer, J.: Kilimanjaro ice core records: Evidence of Holocene climate change in Tropical Africa, Science, 298, 589–593, 2002.

108. Thompson, L. G., Yao, T., Davis, M. E., Henderson, K. A., Mosley-Thompson, E., Lin, P. N., Beer, J., Synal, H. A., Cole-Dai, J., and Bolzan, J. F.: Tropical climate instability: the last glacial cycle from a Qinghai-Tibetan ice core, Science, 276, 1821–1825, 1997.

109. Törnqvist, T. E. and Hijma, M. P.: Links between early Holocene ice-sheet decay, sea-level rise and abrupt climate change, Nat. Geosci., 5, 601–606, 2012.

110. Viau, A. E., Gajewski, K., Sawada, M. C., and Fines, P.: Millennial-scale temperature variations in North America during the Holocene, J. Geophys. Res., 111, D09102, 2006.

111. Wang, C., Lu, H., Zhang, J., Gu, Z., and He, K.: Prehistoric demographic fluctions in China inferred from radiocarbon data and their linkage with climate

https://doi.org/10.5194/cp-2019-89
Preprint. Discussion started: 9 August 2019



change over the past 50000 years. Quaternary Sci. Rev., 98, 45–59, 2014.

112. Wang, Y., Cheng, H., Edwards, R. L., He, Y., Kong, X., An, Z., Wu, J., Kelly, M. J., Dykoski, C. A., and Li, X.: The Holocene Asian Monsoon: Links to solar changes and North Atlantic Climate, Science, 308, 854–857, 2005.

113. Wang, Z., Zhuang, C., Saito, Y., Chen, J., Zhan, Q., and Wang, X.: Early mid-Holocene sea-level change and coastal environmental response on the southern Yangtze delta plain, China: implications for the rise of Neolithic culture, Quaternary Sci. Rev., 35, 51–62, 2012.

114. Weiss, H.: Global megadrought, societal collapse and resilience at 4.2–3.9 ka BP across the Mediterranean and west Asia, PAGES, 24, 62–63, 2016.

115. Wu, W. and Liu, T.: Possible role of the "Holocene Event 3" on the collapse of neolithic cultures around the Central Plain of China, Quaternary Int., 117, 153–166, 2004.

116. Wu, W., Zheng, H., Hou, M., and Ge, Q.: The 5.5 cal ka BP climate event, population growth, circumscription and the emergence of the earliest complex societies in China, Sci. China Earth Sci., 61, 134–148, 2018.

117. Xu, Q., Xiao, J., Nakamura, T., Yang, X., Yang, Z., Liang, W., Iuchi, B., and Yang, S.: Quantitative reconstruction climatic changes of Daihai by pollen data, Mar. Geol. Quaternary Geol., 3, 99–108 (in Chinese), 2003.

118. Yan, Y., Mayewski, P. A., Kang, S., and Meyerson, E.: An ice-core proxy for Antarctic circumpolar zonal wind intensity, Ann. Glaciol., 41, 121–130, 2005.

119. Yu, K. F., Zhao, J. X., Liu, T. S., Wei, G. J., Wang, P. X., and Collerson, K. D.: High-frequency winter cooling and reef coral mortality during the Holocene climatic optimum, Earth Planet. Sc. Lett., 224, 143–155, 2004.

120. Yu, S. Y., Berglund, B. E., Sandgren, P., and Lambeck, K.: Evidence for a rapid sea-level rise 7600 yr ago, Geology, 35, 891–894, 2007.

121. Zdanowicz, C. M., Zielinski, G. A., and Germani, M. S.: Mount Mazama eruption: Calendrical age verified and atmospheric impact assessed, Geology, 27: 621–624, 1999.

122. Zhang, L., Fang, X., Ren, G., and Suo, X.: Environmental changes in the north China farming-grazing transitional zone, Earth Sci. Front., 4, 127–136, 1997 (in Chinese).

123. Zhang, R. and Delworth, T. L.: Simulated tropical response to a substantial weakening of the Atlantic Thermohaline Circulation, J. Climate, 18, 1853–1860, 2005.

124. Zhang, Z., Leduc, G., and Sachs, J. P.: El Niño evolution during the Holocene revealed by a biomarker rain gauge in the Galápagos Islands, Earth Planet. Sc. Lett., 404, 420–434, 2014.

125. Zhao, C., Yu, Z., Ito, E., and Zhao, Y.: Holocene climate trend, variability, and shift documented by lacustrine stable isotope record in the northeastern United States, Quaternary Sci. Rev., 29, 1831–1843, 2010.

126. Zheng, X., Li, A., Kao, S., Gong, X., Frank, M., Kuhn, G., Cai, W., Yan, H., Wan, S., Zhang, H., Jiang, F., Hathome, E., Chen, Z., and Hu, B.: Synchronicity of Kuroshio Current and climate system variability since the Last Glacial Maximum, Earth Planet. Sc. Lett., 452, 247–257, 2016.

127. Zielhofer, C., Fletcher, W. J., Mischke, S., Batist, M. D., Campbell, J. F. E., Joannin, S., Tjallingii, R., Hamouti, N. E., Junginger, A., Stele, A., Bussmann, J., Schneider, B., Lauer, T., Spitzer, K., Strupler, M., Brachert, T., and Mikdad, A.: Atlantic forcing of Western Mediterranean winter rain minima during the last 12,000 years, Quaternary Sci. Rev., 157, 29–51, 2017a.

128. Zielhofer, C., von Suchodoletz, H., Fletcher, W. J., Schneider, B., Dietze, E., Schlegel, M., Schepanski, K., Weninger, B., Mischke, S., and Mikdad, A.: Millennial-scale fluctuations in Saharan dust supply across the decline of the African Humid Period, Quaternary Sci. Rev., 171: 119–135, 2017b.

129. Zielinski, G. A., Mayewski, P. A., Meeker, L. D., Whitlow, S., and Twickler, M. S.: A 110,000-Yr Record of explosive volcanism from the GISP2 (Greenland) ice core, Quaternary Res., 45, 109–118, 1996.

130. Zong, Y., Chen, Z., Innes, J. B., Chen, C., Wang, Z., and Wang, H.: Fire and

https://doi.org/10.5194/cp-2019-89
Preprint. Discussion started: 9 August 2019



flood management of coastal swamp enabled first rice paddy cultivation in east China, Nature, 449, 459–462, 2007.